(12) INTERNATIONAL APPLICATION PUBLISHED UNDER THE PATENT COOPERATION TREATY (PCT)

CORRECTED VERSION

(19) World Intellectual Property Organization
International Bureau

(43) International Publication Date
31 March 2011 (31.03.2011)

PCT

(10) International Publication Number
WO 2011/036676 A8

(51) International Patent Classification:
A61K 31/4188 (2006.01)

(21) International Application Number:
PCT/IN2010/000613

(22) International Filing Date:
14 September 2010 (14.09.2010)

(25) Filing Language: English

(26) Publication Language: English

(30) Priority Data:
2303/CEH/2009 23 September 2009 (23.09.2009) IN

(72) Inventor; and
(71) Applicant : **NANGIA, Ashwini** [IN/IN]; Plot 81 A/C, Unit D, MLA Colony, Road No.12, Banjara Hills, Hyderbad 500 034 (IN).

(72) Inventors; and
(75) Inventors/Applicants *(for US only)*: **NANUBOLU, Jagadeesh, Babu** [IN/IN]; School of Chemistry, University of Hyderabad, Hyderabad 500 046 (IN). **SANPHUI, Palash** [IN/IN]; School of Chemistry, University of Hyderabad, Hyderabad 500 046 (IN).

(74) Agent: **NAIR, Gopakumar, G.**; Patent & Trademark Attorney, Gopakumar Nair Associates, 3rd Floor, Shivmangal, Near Big Bazaar, Akurli Road Kandivali (East) Mumbai 400 101 Maharashtra (IN).

(81) Designated States *(unless otherwise indicated, for every kind of national protection available)*: AE, AG, AL, AM, AO, AT, AU, AZ, BA, BB, BG, BH, BR, BW, BY, BZ, CA, CH, CL, CN, CO, CR, CU, CZ, DE, DK, DM, DO, DZ, EC, EE, EG, ES, FI, GB, GD, GE, GH, GM, GT, HN, HR, HU, ID, IL, IN, IS, JP, KE, KG, KM, KN, KP, KR, KZ, LA, LC, LK, LR, LS, LT, LU, LY, MA, MD, ME, MG, MK, MN, MW, MX, MY, MZ, NA, NG, NI, NO, NZ, OM, PE, PG, PH, PL, PT, RO, RS, RU, SC, SD, SE, SG, SK, SL, SM, ST, SV, SY, TH, TJ, TM, TN, TR, TT, TZ, UA, UG, US, UZ, VC, VN, ZA, ZM, ZW.

(84) Designated States *(unless otherwise indicated, for every kind of regional protection available)*: ARIPO (BW, GH, GM, KE, LR, LS, MW, MZ, NA, SD, SL, SZ, TZ, UG, ZM, ZW), Eurasian (AM, AZ, BY, KG, KZ, MD, RU, TJ, TM), European (AL, AT, BE, BG, CH, CY, CZ, DE, DK, EE, ES, FI, FR, GB, GR, HR, HU, IE, IS, IT, LT, LU, LV, MC, MK, MT, NL, NO, PL, PT, RO, SE, SI, SK, SM, TR), OAPI (BF, BJ, CF, CG, CI, CM, GA, GN, GQ, GW, ML, MR, NE, SN, TD, TG).

Declarations under Rule 4.17:

— *as to applicant's entitlement to apply for and be granted a patent (Rule 4.17(ii))*

— *as to the applicant's entitlement to claim the priority of the earlier application (Rule 4.17(iii))*

— *of inventorship (Rule 4.17(iv))*

Published:

— *without international search report and to be republished upon receipt of that report (Rule 48.2(g))*

(48) Date of publication of this corrected version:
26 May 2011

(15) Information about Correction:
see Notice of 26 May 2011

(54) Title: STABLE COCRYSTALS OF TEMOZOLOMIDE

(57) Abstract: Disclosed herein are novel pharmaceutical cocrystals of temozolomide using co-crystal coformers selected from aliphatic and aromatic carboxylic acids in fixed stoichiometric ratio. The novel Temozolomide-carboxylic acid cocrystals exhibit improved hydrolytic stability and good aqueous dissolution rate compared to the pure drug.

WO 2011/036676 A8

Stable Cocrystals of Temozolomide

Technical field of the invention

The present invention relates to the field of pharmaceutical cocrystals. In particular, the present invention relates to novel pharmaceutical cocrystals of temozolomide (TMZ) with carboxylic acids having a fixed active pharmaceutical ingredient (API) : cocrystal former (CCF) stoichiometry for improved stability and good dissolution rate.

Background of invention

This application claims the benefit of Indian provisional patent application No. 2303/CHE/2009 filed on 23/09/2009.

Pharmaceutical cocrystals are defined as hydrogen bonded complexes between an active pharmaceutical ingredient (API) or a drug molecule and a coformer (CCF) or a benign partner molecule, usually having a fixed API : CCF stoichiometry (Ö. Almarsson, and M. J. Zaworotko, Chem. Commun., 2004, 1889-1896). The utility of pharmaceutical cocrystals in solving stability, solubility, bioavailability, filtration, hydration, tableting, etc. issues are highlighted in the papers by N. Shan, and M. J. Zaworotko, Drug. Disc. Today, 2008, 13, 440-446; A. V. Trask, W. D. S. Motherwell, and W. Jones, Cryst. Growth Des., 2005, 5, 1013-1021; and N. J. Babu, L. S. Reddy, and A. Nangia. Mol. Pharmaceutics, 2007, 4, 417-434. The terms 'cocrystal' and 'molecular complex' are used widely and interchangeably to describe hydrogen bonded structures of the type discussed in this application (M. R. Caira, L. R. Nassimbeni and A. F. Wildervanck, J. Chem. Soc., Perkin Trans. 2, 1995, 2213-2216). The carboxamide group can form cocrystals not only with pyridine-N-oxides (L. S. Reddy, N. J. Babu and A. Nangia, Chem. Commun., 2006, 1369-1371), but also with other functional groups such as carboxylic acid, pyridine, sulfonamide, and carboxamide by applying the rules of hydrogen bond patterns for organic compounds (M. C. Etter, Acc. Chem. Res., 1990, 23, 120-126).

Temozolomide, 8-carbamoyl-3-methylimidazo[5,1-d]-1,2,3,5-tetrazin-4(3H)-one, (TMZ hereafter) is reported as an antitumor agent by P. R. Lowe, C. E. Sansom, C. H. Schwalbe, M. F. G. Stevens, and A. S. Clark, J. Med. Chem., 1992, 35, 3377-3382; and described in US5260291 together with a class of molecules having similar activity (E

Lunt, M. F. G, Stevens, R. Stone, K. R. H. Wooldrdige and E. S. Newlands, US Patent No. 5,260,291, 1993). Temozolomide has the formula given below:

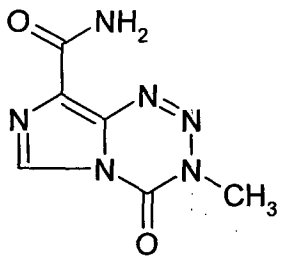

TMZ

Patent Applications Nos. WO/2003/072,082 and US/2006/6,987,108 by S. Ugwu, V. Radhakrishnan, P. M. Ihnat, and L. C. Witchey-Lakshmanan and WO/2008/140,724 by M. Abutarif, and P. Skatkevich relate to pharmaceutical formulation comprising of temozolomide and dissolution enhancing agents such as urea, L-histidine, L-threonine, L-asparagine, L-serine, L-glutamine or mixtures thereof.

Patent Application No.WO/2007/033,374 by C. B. Pickett, W. R. Bishop, and Y. Wang discloses pharmaceutical composition consisting of temozolomide or its pharmaceutically acceptable salt in combination with a protein kinase C (PKC) inhibitor.

Temozolomide belongs to the N-3 substituted carbamoyl imidazo tetrazinone class of drugs (J. M. Malcolm, G. L. Plosker, and B. Jarvis, Am. J. Cancer, 2002, 1, 55-80). This antitumor prodrug is active against malignant melanoma for the treatment of brain tumor. It is an alkylating agent that acts by the water-assisted tetrazinone ring opening to release 3-methyl-(triazenyl-1-yl)imidazole-4-carboxamide (MTIC) through elimination of H2O and loss of CO2. MTIC rapidly degrades to 5-aminoimidazole-4-carboxamide (AIC) and a highly reactive methyldiazonium ion (CH3N2+). Alkylation of guanine in genomic DNA in the major groove results in methylated-DNA adducts (Scheme I). Due to O6-methylguanine lesion being left intact, thymine is re-mismatched leading to cell arrests in the G2/M phase and finally apoptosis (J. C. Baer, A. A. Freeman, E. S. Newlands, A. J. Watson, J. A. Raffetry and G. P. Margison, Br. J. Cancer, 1993, 67, 1299-1302; L. Tentori, L. Orlando, P. M. Lacal, E. Benincasa, I. Faraoni, E. Bonmassar, S. D'Atri and G. Graziani, Mol. Pharmacol., 1997, 52, 249-258). N-7 of guanine is the major alkylation

site of calf thymus DNA in labeling studies (B. J. Denny, R. T. Wheelhouse, M. F. G. Stevens, L. L. H. Tsang and J. A. Slack, Biochemistry, 1994, 33, 9045-9051). Similar to alkylating agents, Temozolomide has a greater antitumor effect if a large population of cells is actively replicating.

Mean elimination half life of temozolomide in plasma concentrations is about 1.8 h (range 1.7-1.9 h) with maximum concentration between 0.33-2 h. Conversion of TMZ to MTIC and AIC is pH dependent and irreversible. In aqueous buffers, TMZ is relatively stable at acidic pH < 4, but rapidly hydrolyses to MTIC at pH > 7. In contrast, MTIC is stable at alkaline pH but rapidly breaks down to AIC at pH < 7 (S. D. Baker, M. Wirth, P. Statkevich, P. Reidenberg, K. Alton, S. E. Sartorius, M. Dugan, D. Cutler, V. Batra, L. B. Grochow, R. C. Donchower and E. K. Rowinsky, Clin. Cancer Res., 1999, 5, 309-317). TMZ has in vitro half life of 1.9 h in phosphate buffer at 37 °C and pH 7.5 (physiological pH 7.4) whereas MTIC has half life of ~2 min. Temozolomide is completely decomposed at pH 9. In time-dependent experiments, TMZ starts to decompose in 5 min at neutral and alkaline pH solutions, whereas 90% of TMZ was intact in acidic medium for 60 min (T. Kodawara, T. Mizuno, H. Taue, T. Hashida, I. Yano, T. Katsura and K. Inui, Yakugaku Zasshi, 2009, 129, 353-357). The effect of temperature was also studied (H. Kim, P. Likhari, D. Parker, P. Statkevich, A. Marco, C.-C. Lin and A. A. Nomeir, J. Pharma, Biomed. Anal., 2001, 24, 461-468). TMZ is unstable at 37 °C in human plasma (pH 7.4) with T½ (half life) of 15 min but stable for at least 30 min at 4 °C. TMZ is stable in acidified human plasma (pH < 4) for at least 24 h at 25 °C and for at least 30 days at –20 °C.

An improved process for the preparation of Temozolomide from Temozolomide hydrochloride avoids strong base for neutralization, such as NaOH, but instead preferably use acetic acid to obtain pure Temozolomide in good yield and purity (Example 2 of O. Etlin, M. Alnabari, Y. Sery, E. Danon, O. Arad, and J. Kaspi, US 2006/0183898, 2006). The structure of temozolomide hydrochloride salt was assigned as shown below by Y. Wang and M. F. G. Stevens et al. in J. Org. Chem., 1997, 62, 7288-7294 (structure 31).

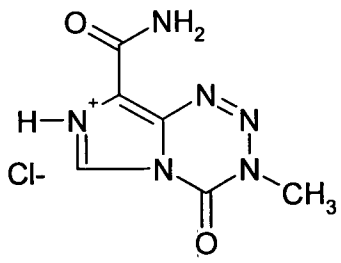

TMZ hydrochloride

Temozolomide tablets are marketed under the brand name Temodor® in USA by Schering-Plough Corporation, Kenilworth, New Jersey and as Temodal® in other markets. According to the teaching of the process patent for the preparation of Temozolomide (Example 1 of US2002/0095036), the compound is obtained as a white precipitate in pure form (S. -C. Kuo, J. L. Mas, and D. Hou, US Patent No. 2002/0095036 A1, 2002). The Temodar® drug leaflet states that the "material is a white to light tan/ light pink powder". The light tan/ pink color is indicative of degradation.

An improved storage system for temozolomide was developed by O. Braverman, R. Felnshtein, A. Welsman, and J. Kaspl, US Patent No.US 2006/0222792 A1, 2006; ibid, Canadian Patent No. CA 2585406 A1, 2007 to prevent the drug from decomposing for prolonged periods. One to three polymeric bags with an optional desiccant in an inert atmosphere is able to keep TMZ as a white solid for 4-6-10 weeks respectively. A sign of TMZ decomposition is change in color from white to pink to traces of tan color. For example, without any protection system, TMZ turned pinkish in 6 weeks but with three layers of sealed package under nitrogen atmosphere and desiccant, the drug remained white at 10 weeks duration. Temozolomide lyophilized material is white to light pink/ light tan powder.

The biochemical mode of action of temozolomide is given in Scheme I.

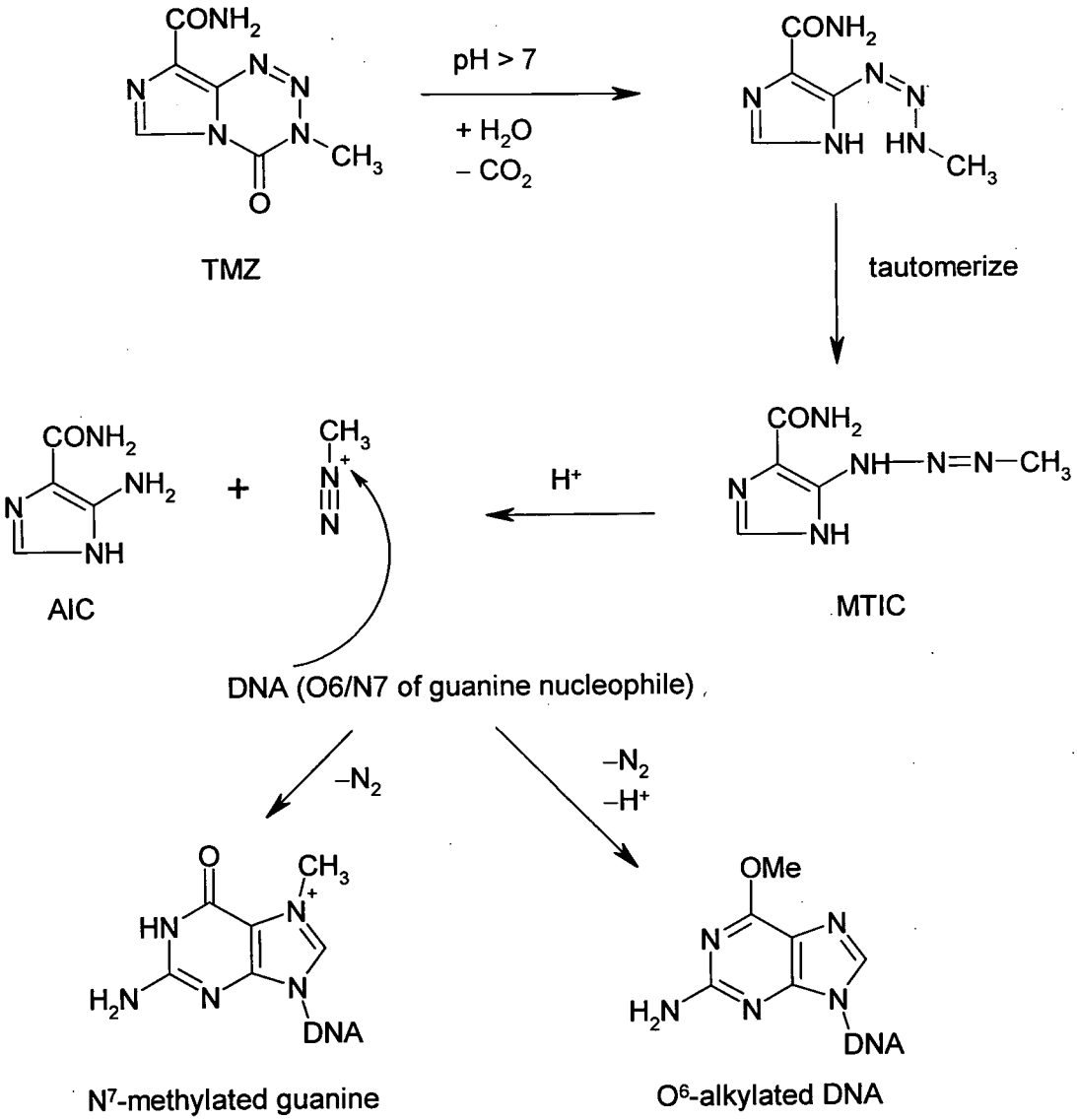

Base pair mismatch

Scheme I: Biochemical mode of action of Temozolomide via hydrolysis to MTIC, which generates methyldiazonium cation active species that alkylates DNA leading to apoptosis. The first two steps are pH dependent.

Further, temozolomide rapidly decomposes in aqueous medium or in presence of high relative humidity. In about 2 months the color of temozolomide (initially pure white) changes to light pink to light tan, suggesting degradation of the API. Temozolomide starts to degrade when crystallized from polar solvents, e.g. water, methanol, ethanol etc. In view of the apparent tendency of temozolomide to degrade, as is evident by a change in

its color, it is necessary to develop Temozolomide in co-crystal form which will increase the stability or shelf life.

Object of the Invention

It is thus the object of the present invention to prepare novel pharmaceutical cocrystals of Temozolomide (TMZ) using co-crystal formers (CCFs) selected from the group of aliphatic and aromatic carboxylic acids in fixed stoichiometric ratio, having improved stability and dissolution rate compared to the pure drug.

Summary of the invention

In accordance with the above objective, the present invention relates to novel cocrystals of temozolomide using suitable co-crystal formers selected from aliphatic and aromatic carboxylic acids in fixed stoichiometric ratio. The carboxylic acids having pKa value in the range of 2 to 6 are used as pH adjusters in the cocrystals.

In an aspect of the present invention, the co-crystal formers are selected from aliphatic and aromatic acids consisting of several mono and dicarboxylic acids such as formic acid, acetic acid, oxalic acid, succinic acid, citric acid, salicylic acid, d,l-malic acid, d,l-tartaric acid, maleic acid, fumaric acid, malonic acid, benzoic acid, crotonic acid, p-hydroxybenzoic acid, p-aminobenzoic acid, anthranilic acid, cinnamic acid, propanoic acid, sorbic acid, linoleic acid, adipic acid, lactic acid , aconitic acid, glutaric acid, etc., specifically with oxalic acid, succinic acid, salicylic acid, d,l-malic acid, anthranilic acid, and d,l-tartaric acid.

In a preferred aspect, cocrystals with succinic acid (1:0.5), oxalic acid (1:0.5), salicylic acid (1:1), d,l-malic acid (1:0.5), anthranilic acid (2:1) and d,l-tartaric acid (1:1) are disclosed .

In another aspect, the co-crystals of temozolomide with carboxylic acids of the instant invention are prepared by solvent-mediated grinding method and further crystallized from laboratory solvents for example, water, methanol, THF, DMF, acetonitrile, etc.

In a further aspect, the precipitated co-crystals were characterized by X-ray powder diffraction, IR and Raman spectroscopy and melting point. UV-Vis spectroscopy study

was performed on temozolomide and its carboxylic acid cocrystals with succinic acid (1:0.5), oxalic acid (1:0.5), salicylic acid (1:1), d,l-malic acid (1:0.5), anthranilic acid (2:1) and d,l-tartaric acid (1:1) to measure degradation rate and hence to compare their stability.

Apart from stability, the bioavailability of a drug is equally important for its therapeutic potential. To measure the apparent solubility of cocrystals of Temozolomide with carboxylic acids, intrinsic dissolution study was performed at physiological pH 7 buffer medium.

In another aspect, the invention provides pharmaceutical compositions comprising a therapeutically effective amount of temozolomide with any one of the co-crystal former as mentioned above along with one or more suitable pharmaceutical carriers /exicipients.

The carriers/ excipients are added to the composition for variety of purposes. Dosage forms include solid dosage forms such as tablets, powders, capsules, liquid dosage forms as well as parenteral dosage forms. The dosage forms can also be prepared as sustained, controlled, modified and immediate dosage forms. The active ingredient(s) and excipients can be formulated into compositions and dosage forms according to methods known in the art.

The invention further discloses use of the 'composition of the invention' in preparing the medicament intended to treat cancer.

Brief description of the Drawings

Figure 1 depicts UV-Vis spectra of Temozolomide at 25 μM concentration in aqueous solution. The time at which TMZ and AIC peak heights are about equal is indicated with an arrow T½.

Figure 2 depicts UV-Vis spectra of Temozolomide–succinic acid (1:0.5) cocrystal at 25 μM concentration in aqueous solution. The time at which TMZ and AIC peak heights are about equal is indicated with an arrow T½.

Figure 3 depicts UV-Vis spectra of Temozolomide–oxalic acid (1:0.5) cocrystal at 25 μM concentration in aqueous solution. The time at which TMZ and AIC peak heights are about equal is indicated with an arrow T½.

Figure 4 depicts UV-Vis spectra of Temozolomide–salicylic acid (1:1) cocrystal at 25 μM concentration in aqueous solution. The time at which TMZ and AIC peak heights are about equal is indicated with an arrow T½.

Figure 5 depicts UV-Vis spectra of Temozolomide at 10 μM concentration in pH 7 buffer solution. The time at which TMZ and AIC peak heights are about equal is indicated with an arrow T½.

Figure 6 depicts UV-Vis spectra of Temozolomide–succinic acid (1:0.5) cocrystal at 10 μM concentration in pH 7 buffer solution. The time at which TMZ and AIC peak heights are about equal is indicated with an arrow T½.

Figure 7 depicts UV-Vis spectra of Temozolomide–oxalic acid (1:0.5) cocrystal at 10 μM concentration in pH 7 buffer solution. The time at which TMZ and AIC peak heights are about equal is indicated with an arrow T½.

Figure 8 depicts UV-Vis spectra of Temozolomide–salicylic acid (1:1) cocrystal at 10 μM concentration in pH 7 buffer solution. The time at which TMZ and AIC peak heights are about equal is indicated with an arrow T½.

Figure 9 depicts UV-Vis spectra of Temozolomide–d,l-malic acid (1:0.5) cocrystal at 10 μM concentration in pH 7 buffer solution. The time at which TMZ and AIC peak heights are about equal is indicated with an arrow T½.

Figure 10 depicts UV-Vis spectra of Temozolomide–anthranilic acid (2:1) cocrystal at 10 μM concentration in pH 7 buffer solution. The time at which TMZ and AIC peak heights are about equal is indicated with an arrow T½.

Figure 11 depicts UV-Vis spectra of Temozolomide–d,l-Tartaric acid (1:1) cocrystal at 10 μM concentration in pH 7 buffer solution. The time at which TMZ and AIC peak heights are about equal is indicated with an arrow T½.

Figure 12 depicts X-ray powder diffraction of Temozolomide used in co-crystallization experiments.

Figure 13 depicts X-ray powder diffraction of Temozolomide–oxalic acid cocrystal (1:0.5).

Figure 14 depicts X-ray powder diffraction of Temozolomide–succinic acid cocrystal (1:0.5).

Figure 15 depicts X-ray powder diffraction of Temozolomide–salicylic acid cocrystal (1:1).

Figure 16 depicts X-ray powder diffraction of Temozolomide–d,l-malic acid cocrystal (1:0.5).

Figure 17 depicts X-ray powder diffraction of Temozolomide–anthranilic acid cocrystal (2:1).

Figure 18 depicts X-ray powder diffraction of Temozolomide–d,l-Tartaric acid cocrystal (1:1).

Figure 19 depicts FT-IR spectra of Temozolomide–succinic acid cocrystal (1:0.5), Temozolomide form used, and succinic acid.

Figure 20 depicts FT-IR spectra of Temozolomide–oxalic acid cocrystal (1:0.5), Temozolomide form used, and oxalic acid.

Figure 21 depicts FT-IR spectra of Temozolomide–salicylic acid cocrystal (1:1), Temozolomide form used, and salicylic acid.

Figure 22 depicts FT-IR spectra of Temozolomide–d,l-malic acid cocrystal (1:0.5), Temozolomide form used, and d,l-malic acid.

Figure 23 depicts FT-IR spectra of Temozolomide–anthranilic acid cocrystal (2:1), Temozolomide form used, and anthranilic acid.

Figure 24 depicts FT-IR spectra of Temozolomide–d,l-tartaric acid cocrystal (1:1), Temozolomide form used, and d,l-Tartaric acid.

Figure 25 depicts FT-Raman spectra of Temozolomide–succinic acid cocrystal (1:0.5), Temozolomide form used, and succinic acid.

Figure 26 depicts FT-Raman spectra of Temozolomide–oxalic acid cocrystal (1:0.5), Temozolomide form used, and oxalic acid.

Figure 27 depicts FT-Raman spectra of Temozolomide–salicylic acid cocrystal (1:1), Temozolomide form used, and salicylic acid.

Figure 28 depicts FT- Raman spectra of Temozolomide–d,l-malic acid cocrystal (1:0.5), Temozolomide form used, and d,l-malic acid.

Figure 29 depicts FT-Raman spectra of Temozolomide–anthranilic acid cocrystal (2:1), Temozolomide form used, and anthranilic acid.

Figure 30 depicts FT-Raman spectra of Temozolomide–d,l-Tartaric acid cocrystal (1:1), Temozolomide form used, and d,l-Tartaric acid.

Figure 31 depicts DSC thermogram of Temozolomide–oxalic acid cocrystal (1:0.5).

Figure 32 depicts DSC thermogram of Temozolomide–succinic acid cocrystal (1:0.5).

Figure 33 depicts DSC thermogram of Temozolomide–salicylic acid cocrystal (1:1).

Figure 34 depicts DSC thermogram of Temozolomide–d,l-malic acid cocrystal (1:0.5).

Figure 35 depicts DSC thermogram of Temozolomide–anthranilic acid cocrystal (2:1).

Figure 36 depicts DSC thermogram of Temozolomide–d,l-Tartaric acid cocrystal (1:1).

Figure 37 depicts the ORTEP diagram (at 35% probability for heavy atoms) and hydrogen bonding in unit cell of Temozolomide–oxalic acid cocrystal (1:0.5).

Figure 38 depicts the ORTEP diagram (at 35% probability for heavy atoms) and hydrogen bonding in unit cell of Temozolomide–succinic acid cocrystal (1:0.5).

Figure 39 depicts the ORTEP diagram (at 35% probability for heavy atoms) and hydrogen bonding in unit cell of Temozolomide–salicylic acid cocrystal (1:1).

Figure 40 depicts the ORTEP diagram (at 35% probability for heavy atoms) and hydrogen bonding in unit cell of Temozolomide–d,l-malic acid cocrystal (1:0.5). O6 atom of Malic acid is disordered over two positions with equal site occupancy factor of 0.5.

Figure 41 depicts the ORTEP diagram (at 35% probability for heavy atoms) and hydrogen bonding in unit cell of Temozolomide–anthranilic acid cocrystal (2:1).

Figure 42 depicts the ORTEP diagram (at 35% probability for heavy atoms) and hydrogen bonding in unit cell of Temozolomide–d,l-Tartaric acid cocrystal (1:1).

Figure 43 depicts Comparison of intrinsic dissolution rate of Temozolomide (trace 1, ▲) and six cocrystals in pH 7 aqueous buffer medium: Temozolomide–oxalic acid (1:0.5) (trace 2, □), Temozolomide–succinic acid (1:0.5) (trace 3, ⊖), Temozolomide–salicylic acid (1:1) (trace 4, Δ), Temozolomide–d,l-malic acid (1:0.5) (trace 5, ♦), Temozolomide–anthranilic acid (2:1) (trace 6, *), Temozolomide–d,l-tartaric acid (1:1) (trace 7, ⛒).

Detailed Description of the Invention

The invention will now be described in detail in connection with certain preferred and optional embodiments, so that various aspects thereof may be more fully understood and appreciated.

"Co-crystal and cocrystal refer to hydrogen bonded molecular complex".

"The names d,l-malic acid or malic acid and d,l-tartaric acid or tartaric acid mean one and the same chemical".

The present invention relates to novel co-crystals of temozolomide prepared using co-crystal formers selected from aliphatic and aromatic carboxylic acid in fixed stoichiometric ratio to enhance the stability and dissolution rate of the parent anti tumor prodrug temozolomide. Further, the novel cocrystals of the present invention works along with parent anti-tumor prodrug, temozolomide, thus enhancing the efficacy of the parent molecule in lower doses.

Temozolomide (TMZ) is an oral alkylating agent which can be used for the treatment of various grades of tumor. A derivative of imidazotetrazine, temozolomide is the prodrug of MTIC (3-methyl-(triazen-1-yl)imidazole-4-carboxamide). Temozolomide, an antitumor drug, begins to degrade in aqueous medium at pH 6.0, and the decomposition is faster at higher physiological basic pH (~7.4). In order to improve its stability due to hydrolytic decomposition, the present inventors have developed novel pharmaceutical cocrystals of Temozolomide, using co-crystal formers selected from aliphatic and aromatic carboxylic acids in fixed stoichiometric ratio. The carboxylic acids having pKa value in the range of 2 to 6 are used as pH adjusters in the cocrystals to maintain the crystalline environment acidic enough for temozolomide molecules to improve their hydrolytic stability.

The aliphatic and aromatic carboxylic acids used as co-crystal formers are selected from several mono and dicarboxylic acids such as formic acid, acetic acid, oxalic acid, succinic acid, salicylic acid, d,l-malic acid, d,l-tartaric acid, maleic acid, citric acid, fumaric acid, cinnamic acid, malonic acid, benzoic acid, crotonic acid, p-hydroxybenzoic acid, p-aminobenzoic acid, anthranilic acid propanoic acid, sorbic acid, linoleic acid, adipic acid, lactic acid , aconitic acid, glutaric acid, etc., specifically oxalic acid, succinic acid, salicylic acid, d,l-malic acid, anthranilic acid, and d,l-tartaric acid.

Accordingly in a preferred embodiment, the present invention discloses novel pharmaceutical cocrystals comprising of temozolomide as API and a carboxylic acid coformer having a fixed stoichiometric ratio, such as the cocrystals of temozolomide with succinic acid (1:0.5), oxalic acid (1:0.5), salicylic acid (1:1), d,l-malic acid (1:0.5), anthranilic acid (2:1) and d,l-tartaric acid (1:1).

The pharmaceutical cocrystals of TMZ with the above mentioned carboxylic acids as coformers are found to bring down pH levels <5 during crystallization, thereby suppressing degradation of TMZ thus improving its stability and shelf life.

The invention further provides a process for preparing the cocrystal of the present invention, involving solvent drop grinding method (A. V. Trask, W. D. S. Motherwell, and W. Jones, Chem. Commun., 2004, 890-891; A. V. Trask, and W. Jones, Top. Curr. Chem., 2005, 254, 41-70). Accordingly, Temozolomide and carboxylic acid coformers selected from the group consisting of succinic acid , oxalic acid, salicylic acid, d,l-malic acid, anthranilic acid, and d,l-tartaric acid are taken in a definite stoichiometric ratio and grinded in a mortar-pestle for 15 minutes with drop wise addition of acetonitrile. Further, the cocrystals of temozolomide are crystallized from common laboratory solvents, e.g. water, methanol, acetonitrile, DMF, tetrahydrofuran or dioxane and the like, under ambient conditions. The crystallization process and the conditions are described in Table 1 below.

It is observed that the cocrystals of TMZ with carboxylic acid coformers crystallized from polar solvents such as water, methanol and ethanol, and did not show any appreciable hydrolysis of TMZ even after a week long period of crystallization. These results suggested that the degradation of TMZ was suppressed and its stability improved due to the coformers. As a result, TMZ–oxalic acid, TMZ–salicylic acid, TMZ–succinic acid, TMZ–d,l-malic acid, TMZ–anthranilic acid, TMZ–d,l-tartaric acid cocrystals could be stored as crystalline material for several months under ambient conditions without any sign of decomposition.

In another embodiment, these cocrystals which precipitated out of solution after 2-3 days, and in other cases after 4-5 days, were analyzed and characterized by X-ray powder diffraction (XRPD), FT-IR, FT-Raman spectroscopy and Differential Scanning Calorimetry (DSC). Their stability in water as well as in physiological pH 7 aqueous buffer medium is monitored by UV-Vis spectroscopy and described.

Significant differences in IR, Raman, XRPD and melting point which suggests the formation of new solid phase in each case is as described herein below. Further, UV-Vis

spectroscopic studies showed that oxalic acid, salicylic acid and succinic acid coformers are superior to make TMZ cocrystals for improved hydrolytic stability. Again pharmaceutical cocrystal TMZ–d,l-malic acid and TMZ–salicylic acid have good stability when coformers from the safe list of GRAS chemicals is considered (GRAS is generally regarded as safe chemicals of the US-FDA).

In another embodiment, the decomposition study of cocrystals of TMZ with succinic acid, oxalic acid, salicylic acid, d,l-malic acid, anthranilic acid, and d,l-tartaric acid is performed in aqueous medium at room temperature and at 25 μM concentration, as well as in physiological pH 7 buffer medium at 10 μM concentration at 37 °C to compare the stability with respect to TMZ.

The half life of temozolomide at 25 μM concentration in aqueous medium at room temperature is 47 h, whereas that for cocrystals with succinic acid, oxalic acid and salicylic acid T½ increases to 86 h, 135 h and 143 h respectively under the same conditions of solvent, concentration and temperature.

The human plasma concentration of Temozolomide drug is 10 μM. The half life of TMZ and its cocrystals measured by UV-Vis spectroscopy at 10 μM concentration in physiological pH 7 buffer at 37 °C is 1.7 h. T½ for cocrystals of TMZ with succinic acid, oxalic acid, salicylic acid, d,l-malic acid, anthranilic acid and d,l-tartaric acid cocrystals is 2.3 h, 3.5 h, 3.6 h, 2.7 h, 2.2 h and 2.5 h respectively at the same concentration, buffer medium and temperature.

The utility cocrystals as a means to improve the solubility of solid forms of drugs are reported in the published literature (N. Blagden, M. de Matas, P. T. Gavan and P. Cork, Adv. Drug. Delivery Rev., 2007, 59, 617-630) and prior art (M. Hanna, N. Shan, M. L. Cheney and D. R. Weyna, US Patent No.US 2009/0203680 A1, 2009).

In another embodiment, the intrinsic solubility of Temozolomide cocrystals is measured. TMZ–oxalic acid (1:0.5) and TMZ–succinic acid (1:0.5) cocrystals have comparable intrinsic dissolution rate to that of pure TMZ up to 150 min. TMZ–salicylic acid (1:1) and TMZ–malic acid (1:0.5) showed solubility profile better than other cocrystals of TMZ

after 60 min. TMZ–tartaric acid (1:1) showed comparable dissolution rate to TMZ up to 60 min and then the rate is slower.

In yet another embodiment, the pKa values of the TMZ–carboxylic acid cocrystals are assessed for their stability and it is observed that all the co-crystals according to the invention are stable. The pKa value of the coformers succinic acid are 4.2, 5.6; oxalic acid 2.1, 4.2; salicylic acid 2.9, d,l-malic acid 3.5, 5.1, d,l-tartaric acid 3.2, 4.8 and anthranilic acid 4.95, respectively (one pKa value for monoacids and 1st and 2nd pKa for diacids). Thus cocrystals of TMZ with pH adjusters maintained the environment acidic so that the hydrolytic stability of Temozolomide is improved. TMZ-Cocrystals are stabilized by the acidity of the coformer, here the carboxylic acid.

pH adjusters are reported in the published literature to improve solubility of Fenoldopam (K. Thoma and I. Ziegler, Eur. J. Pharm. Biopharm., 1998, 46, 105-113) and to increase the shelf-life of local anesthetics (M. G. Reichert, and J. Butterworth, Techniques in Regional Anesthesia and Pain Management, 2004, 8, 106-109) and known in the prior art to maintain amiodarone parenteral solution in the pH range 2.5-4.5 (J. E. Kipp, M. J. Doty, C. L. Rebbeck, and J. Y. Eilert, US 6,479,541 B1, 2002) and provide a method to tune the solubility and dissolution rate of APIs via cocrystals at different pH (N. Rodriguez-Hornedo, US 2008/0,132,419 A1, 2008).

In another embodiment, this invention relates to pharmaceutical compositions comprising a therapeutically effective amount of a temozolomide with any one of the co-crystal former as mentioned above along with one or more suitable pharmaceutical carriers / exicipients. Further, the pharmaceutical composition of the invention may be any pharmaceutical form which contains the crystalline form of the cocrystal of the invention. The pharmaceutical composition may be a solid form such as tablets, powders, capsules, a liquid suspension or an injectable composition, along with any suitable carrier well known in the prior art. The dosage forms can also be prepared as sustained, controlled, modified and immediate dosage forms.

Suitable excipients and the amounts to use may be readily determined by the formulation scientist based upon experience and consideration of standard procedures and reference

works in the field, e.g., the buffering agents, sweetening agents, binders, diluents, fillers, lubricants, wetting agents, disintegrants, etc.

A further aspect of the invention relates to the use of a co-crystal as anti neoplastic agent especially for treating brain tumor, skin cancer and various grades of tumor. This use is provided in the form of a medicament or a pharmaceutical composition according to the invention as described above.

In another embodiment, the present invention relates to administering 'an effective amount' of the 'composition of invention ' to the subject suffering from said disease. Accordingly, Temozolomide cocrystals and pharmaceutical compositions containing them may be administered using any amount, any form of pharmaceutical composition via any route of administration effective for the treatment. After formulation with an appropriate pharmaceutically acceptable carrier in a desired dosage, as known by those of skill in the art, the pharmaceutical compositions of this invention can be administered by any means that delivers the active pharmaceutical ingredient (s) to the site of the body whereby it can exert a therapeutic effect on the patient.

Examples of further embodiments of the disclosure described herein are indicated below without, however, being limiting in nature.

Examples

Example 1

Preparation of novel temozolomide cocrystals

Temozolomide was procured from commercial suppliers and used as such. This solid corresponds to essentially pure form I as described in P. R Lowe, C. E. Sansom, C. H. Schwalbe, M. F. G. Stevens, and A. S. Clark, J. Med. Chem., 1992, 35, 3377-3382.

TMZ and carboxylic acid coformers were taken in a definite stoichiometric ratio and grinded in a mortar-pestle for 15 minutes with the drop wise addition of acetonitrile. The final mixture was characterized by FT-IR, FT-Raman spectroscopy, and XRPD and then crystallized from water, methanol or acetonitrile. Crystallization conditions for representative cocrystals preparation are given in Table 1. A few cocrystals were obtained in hydrate form and characterized as such.

Table 1 Carboxylic acid coformers used to crystallize cocrystals of Temozolomide

Cocrystal	Temozolomide TMZ	Cocrystal former CCF	Solvent/ Conditions	Time (days)
Monohydrate of TMZ–Formic acid (2:1)	50 mg (0.26 mmol)	Formic acid	2-4 mL Formic acid	4-5
TMZ–Acetic acid (1:1)	50 mg (0.26 mmol)	Acetic acid	2-4 mL of Acetic acid	4-5
TMZ–Oxalic acid (1:0.5)	40 mg (0.21 mmol)	9.5 mg (0.105 mmol) Oxalic acid	9 mL of CH3CN or 5 mL water	2-3
TMZ–Succinic acid (1:0.5)	50 mg (0.26 mmol)	15.5 mg (0.13 mmol) Succinic acid	8 mL of MeOH or 5 mL water	4-5
TMZ–d,l-Malic acid (1:0.5)	50 mg (0.26 mmol)	17 mg (0.13 mmol) d,l–Malic acid	5 mL water	2-3
Monohydrate of TMZ–p-Aminobenzoic acid (3:1)	40 mg (0.21 mmol)	28 mg (0.21 mmol) PABA	5 mL CH3CN	2-3
Monohydrate of TMZ–Fumaric acid (1:0.5)	50 mg (0.26 mmol)	14.5 mg (0.13 mmol) Fumaric acid	11 mL of CH3CN Pink colored crystals	2-3
TMZ–Salicylic acid (1:1)	50 mg (0.26 mmol)	46 mg (0.26 mmol) Aspirin	7 mL of CH3CN Aspirin hydrolyzed to SA	1-2
TMZ–Salicylic acid (1:1)	50 mg (0.26 mmol)	36 mg (0.26 mmol) Salicylic acid	5 mL of water or CH3CN	2-3
TMZ–Anthranilic acid (2:1)	40 mg (0.21 mmol)	28.8 mg (0.21 mmol) anthranilic acid	10 mL of CH3CN	4-5

TMZ–d,l-Tartaric acid (1:1)	40 mg (0.21 mmol)	31.5 mg (0.21 mmol) d,l-Tartaric acid	10 mL of CH3CN	4-5

All starting materials are stable to the crystallization conditions except aspirin which hydrolyzed in situ to give a 1:1 cocrystal of TMZ with salicylic acid. The same TMZ–salicylic acid (1:1) cocrystal was prepared by taking molar amount of TMZ and salicylic acid. The crystalline solids obtained were characterized by XRPD, DSC, FT-IR, m.p. The resulting stoichiometry of cocrystals was the same whether starting materials were taken in 1:1 or 2:1 ratio and up to 3:1 ratio of TMZ : coformer.

Example 2

Solid state characterization

a) X-ray Powder Diffraction (XRPD)

X-ray powder diffraction of cocrystals prepared by grinding is a standard method for the characterization of resulting solid-state form. The formation of cocrystal was monitored by the appearance of new diffraction peaks. XRPDs were recorded on a PANlytical 1830 (Philips Analytical) diffractometer using Cu-Kα X-radiation (λ = 1.5406 Å) at 35 kV and 25 mA. Figure 12 is XRPD of Temozolomide used in experiments. The appearance of new diffraction peaks indicates the formation of a new phase in each case. Figure 13 is XRPD of Temozolomide–oxalic acid (1:0.5) cocrystal. Figure 14 is XRPD of Temozolomide–succinic acid (1:0.5) cocrystal. Figure 15 is XRPD of Temozolomide–salicylic acid (1:1) cocrystal.

The powder X-ray diffraction of Temozolomide (Figure 12) exhibits characteristic reflections at about 2θ 10.87, 14.75, 26.64, 28.88 and 29.89 ±0.2° (Table 2).

The powder X-ray diffraction of Temozolomide–oxalic acid (1:0.5) cocrystal (Figure 13) exhibits characteristic reflections at about 2θ 9.22, 14.76, 15.79, 18.01, 22.73 and 27.82 ±0.2° (Table 2).

The powder X-ray diffraction of Temozolomide–succinic acid (1:0.5) cocrystal (Figure 14) exhibits characteristic reflections at about 2θ 8.03, 15.71, 16.08, 26.13 and 36.27 ±0.2° (Table 2).

The powder X-ray diffraction of Temozolomide–salicylic acid (1:1) cocrystal (Figure 15) exhibits characteristic reflections at about 2θ 11.31, 14.61, 25.69, 26.65 and 28.48 ±0.2° (Table 2).

The powder X-ray diffraction of Temozolomide–d,l-Malic acid (1:0.5) cocrystal (Figure 16) exhibits characteristic reflections at about 2θ 15.93, 18.59, 20.20, 23.67, 25.47, 25.82 and 26.78 ±0.2° (Table 2).

The powder X-ray diffraction of Temozolomide–anthranilic acid (2:1) cocrystal (Figure 17) exhibits characteristic reflections at about 2θ 5.65, 11.21, 15.23, 23.43, 26.53 and 27.68 ±0.2° (Table 2).

The powder X-ray diffraction of Temozolomide–d,l-tartaric acid (1:1) cocrystal (Figure 18) exhibits characteristic reflections at about 2θ 10.34, 20.61, 24.39, 26.24, 27.38 and 29.07 ±0.2° (Table 2).

Table 2: X-ray powder diffraction lines of temozolomide, temozolomide–succinic acid (1:0.5), temozolomide–oxalic acid (1:0.5), temozolomide–salicylic acid (1:1), temozolomide–d,l-malic acid (1:0.5), temozolomide–anthranilic acid (2:1) and temozolomide–d,l-tartaric acid (1:1) cocrystals characterized by 2θ angle (°), d values (Å) and relative intensity (%).

Temozolomide			TMZ–oxalic acid (1:0.5)		
Angle 2θ (°)	d value (Å)	Relative Intensity (%)	Angle 2θ (°)	d value (Å)	Relative Intensity (%)
10.87	8.12	8.14	9.22	9.57	1.47
13.42	6.59	2.77	12.21	7.24	0.45
14.75	5.99	100.00	13.75	6.43	1.37
16.33	5.42	2.56	14.76	5.99	1.79
18.07	4.90	7.52	15.79	5.60	1.91
19.15	4.63	5.41	16.68	5.31	0.87
21.51	4.13	4.34	18.01	4.92	5.18
21.73	4.08	4.02	21.04	4.22	0.94
23.87	3.72	2.89	22.73	3.91	4.11

26.64	3.34	11.89	23.93	3.71	1.36
27.84	3.20	2.67	24.43	3.64	1.64
28.88	3.08	11.09	25.86	3.44	1.10
29.66	3.0	5.93	26.54	3.35	1.41
29.89	2.98	6.73	27.82	3.20	100.00
30.42	2.93	3.22	28.55	3.12	1.55
32.41	2.76	2.87	29.02	3.07	0.76
32.81	2.73	1.58	29.55	3.02	0.68
35.78	2.51	1.53	30.51	2.93	0.86
41.97	2.15	1.00	33.85	2.64	0.50
44.40	2.04	0.97	36.94	2.43	0.58
47.87	1.89	1.43	39.03	2.30	0.96

TMZ–succinic acid (1:0.5)			TMZ–salicylic acid (1:1)		
Angle (2θ)	d value (Å)	Relative Intensity (%)	Angle (2θ)	d value (Å)	Relative Intensity (%)
8.03	11.00	90.19	7.23	12.21	3.13
15.71	5.63	100.00	11.31	7.81	18.21
16.08	5.51	78.03	14.61	6.05	100.00
18.21	4.86	14.64	15.62	5.67	5.19
18.51	4.79	14.35	21.80	4.07	2.81
20.00	4.43	10.15	25.69	3.46	14.90
21.06	4.21	13.49	26.65	3.34	55.68
24.19	3.67	26.95	28.48	3.13	42.33
24.54	3.62	12.30	29.37	3.04	3.55
26.13	3.41	86.06	31.61	2.83	5.19
27.59	3.23	27.36	32.97	2.71	4.5
28.55	3.12	70.12	34.21	2.62	3.49
29.73	3.0	7.28	35.20	2.54	5.88
30.59	2.92	13.07	38.42	2.34	2.55
32.82	2.72	25.97	40.65	2.22	1.89

35.01	2.56	8.89	46.60	1.95	0.86
36.27	2.47	27.05			
37.52	2.39	5.21			
40.84	2.21	10.66			
42.85	2.11	21.36			
47.56	1.91	11.16			

TMZ–d,l-malic acid (1:0.5)			TMZ–anthranilic acid (2:1)		
Angle (2θ)	d value (Å)	Relative Intensity (%)	Angle (2θ)	d value (Å)	Relative Intensity (%)
7.97	11.08	29.22	5.65	15.61	6.06
15.93	5.56	85.33	11.21	7.88	11.21
18.18	4.87	30.48	13.18	6.71	4.20
18.59	4.76	40.18	15.23	5.81	10.30
20.20	4.39	44.92	15.98	5.54	3.36
22.08	4.02	16.24	17.39	5.09	5.45
23.67	3.75	44.13	18.59	4.76	3.87
25.47	3.49	35.9	19.30	4.59	5.48
25.82	3.44	90.78	22.10	4.02	4.82
26.78	3.32	100.0	22.52	3.94	2.74
27.35	3.25	16.83	23.43	3.79	11.96
30.23	2.95	55.54	25.92	3.43	2.33
32.1	2.78	16.13	26.53	3.36	14.65
32.6	2.74	32.63	27.09	3.28	6.71
35.72	2.51	18.57	27.68	3.22	100.0
37.55	2.39	14.49	33.54	2.67	3.21
			41.05	2.19	4.64

TMZ–d,l-tartaric acid (1:1)		
Angle (2θ)	d value (Å)	Relative Intensity

		(%)
10.34	8.54	25.23
12.07	7.32	8.55
12.51	7.06	9.42
13.88	6.37	10.32
17.65	5.02	8.25
19.13	4.63	7.11
19.74	4.49	16.04
20.61	4.30	31.64
21.32	4.16	10.40
23.39	3.79	9.02
24.39	3.64	40.21
26.24	3.39	21.24
27.38	3.25	85.88
27.89	3.19	15.16
29.07	3.07	100.0
30.76	2.90	6.50

b) FT-IR spectroscopy analysis

Infrared spectroscopy provides information on the vibrational modes of a compound. This is an absorption phenomenon. IR spectra were recorded on samples dispersed in KBr pellets on a Nicolet 6700 FT-IR spectrometer. In general, IR energy is absorbed by polar functional groups, such as amide carbonyl C=O stretch at 1679 cm–1, amide N–H stretch at 3421 cm–1 (asymmetric) and 3388 cm–1 (symmetric) for Temozolomide. The carboxylic acid group of coformer shows C=O stretch in the region of 1720-1706 cm–1. So during cocrystal formation both carbonyl and amide frequencies are expected to change due to formation of hydrogen bonding between the amide group of temozolomide and the carboxylic acid of the coformer (S. L. Johnson and K. A. Rumon, J. Phys. Chem., 1965, 69, 74-86; B. H. Stuart, Infrared Spectroscopy: Fundamentals and Applications, 2004, John-Wiley, UK). IR comparison of TMZ–carboxylic acid cocrystals along with coformer and parent API are shown in Figure 19-24 to characterize new solid-state cocrystals and the characteristic frequencies are listed in Table 3.

Table 3: FT-IR vbar (cm–1) of TMZ and its cocrystals.

	N–H stretching	C=O stretching	N–H bend	C–O stretch	C–N stretch
TMZ	3421.8, 3388.6, 3287.0	1758.3, 1733.8, 1679.2	1601.5	1218.6	1354.5
TMZ–succinic acid (1:0.5)	3434.9, 3295.5, 3246.3	1731.7, 1686.2	1590.5	1200.8	1366.2
TMZ–oxalic acid (1:0.5)	3403.0, 3256.1 (br.)	1749.7, 1710.7	1592.6	1219.5	1359.1
TMZ–salicylic acid (1:1)	3432.8, 3322.2	1754.4, 1677.4	1578.0	1227.8	1366.7
TMZ–dl-malic acid (1:0.5)	3412.0, 3302.7, 3230.1	1735.9, 1692.2	1587.8	1224.7	1363.8
TMZ–anthralinic acid (2:1)	3439.2, 3329.3, 3183.3, 3126.4	1751.2, 1668.5	1585.8	1239.9	1362.3
TMZ–dl-tartaric acid (1:1)	3452.3, 3341.6, 3132.9	1750.4, 1701.2, 1650.1	1591.3	1222.2	1360.6

A change in both carbonyl and amide stretching frequencies in the IR spectra of TMZ–carboxylic acid cocrystals compared to individual components shows the formation of new solid phase (cocrystal). Solid state grinding of TMZ and carboxylic acid partner molecule in mortar pestle in the presence of a few drops of acetonitrile gave the requisite cocrystal. X-ray quality single crystals could be grown by dissolving the ground mixture in water / acetonitrile solvents and leaving the solution to crystallize.

c) FT-Raman spectroscopy analysis

Raman spectroscopy provides information on the vibrational modes of a compound (R. L. McCreery, Raman Spectroscopy for Chemical Analysis, John-Wiley, 2000, UK; E. Smith and G. Dent, Modern Raman Spectroscopy - A Practical Approach, John-Wiley, 2005, UK). This technique is based on scattering phenomenon. Raman spectra were recorded in a standard NMR tube on Nicolet 6700 FT-Raman spectrometer using Nd:YAG laser (1064 nm). The radiation is more effectively scattered in the Raman Effect by symmetric

vibrations and nonpolar groups. Unlike IR, in Raman the non-polar functional groups (such as C–C) are more intense whereas polar functional groups (such as C–O, C–N) have lower intensity. The frequency of course remains the same as in IR spectrum. Thus amide carbonyl appears at 1672 cm–1, C–N stretch at 1340-1350 cm–1, N–H bend at 1580 cm–1. So during cocrystal formation both carbonyl and amide frequencies are expected to change due to formation of new solid adduct between temozolomide and carboxylic acid. Raman spectra comparison of TMZ–carboxylic acid cocrystals along with coformer and the parent drug are shown in Figures 25-30. Stretching frequencies in the Raman spectra of TMZ and its cocrystals are listed in Table 4.

Table 4: FT-Raman νbar (cm–1) of TMZ and its cocrystals.

	C–H stretching	C=O stretching	N–H bend	C–O strech	C–N strech
TMZ	3115.6, 2966.0	1732.5,1671.9	1576.4	1224.2	1340.9, 1355.7
TMZ–succinic acid (1:0.5)	3110.3, 2957.2, 2932.6	1731.8	1582.4	1210.8, 1225.2	1341.8, 1361.7
TMZ–oxalic acid (1:0.5)	3098.2, 2966.0	1746.3	1582.6	1220.7	1357.0
TMZ–salicylic acid (1:1)	3124.2, 3066.9, 2964.5	1757.3, 1635.6	1607.3, 1575.9	1225.8	1366.8
TMZ–dl-malic acid (1:0.5)	3107.2, 2954.8	1733.0	1577.5	1226.2	1359.9
TMZ–anthralinic acid (2:1)	3124.2, 3085.7, 2955.2	1755.0, 1661.8,	1611.6, 1581.0	1229.9	1357.0 1346.2
TMZ–dl-tartaric acid (1:1)	3131.8, 2952.5	1756.8, 1741.3	1585.8	1221.5	1357.1

d) Thermal analysis of TMZ carboxylic acid cocrystals

Differential scanning calorimetry (DSC) was carried out to investigate the thermal behavior of six TMZ–carboxylic acid cocrystals. DSC shows the exotherm or endotherm at which the solid sample decomposes or melts, respectively. DSC was performed on

Mettler Toledo DSC 822e module by placing the samples, typically 4-6 mg, in aluminum pans and heated in the temperature range 30-250°C @ 5 °C /min. From the area of the exotherm or endotherm peak, enthalpy of fusion (ΔHf) can be calculated. From Fisher-Jones melting point apparatus, it was confirmed that all cocrystals and also the parent API Temozolomide decompose during heating below the decomposition temperature of TMZ (210°C). DSC exotherm, i.e. heat evolution, indicate decomposition of cocrystals. DSC thermograms of cocrystals are shown in Figures 31-36.

DSC of TMZ–oxalic acid cocrystal (1:0.5) shows an exotherm at 176 °C, corresponding to decomposition (Figure 31).

DSC of TMZ–succinic acid cocrystal (1:0.5) shows an exotherm at 180°C, corresponding to decomposition (Figure 32).

DSC of TMZ–salicylic acid cocrystal (1:1) shows an exotherm at 173 °C, corresponding to decomposition (Figure 33).

DSC of TMZ–d,l-malic acid cocrystal (1:0.5) shows an exotherm at 169°C, corresponding to decomposition (Figure 34).

DSC of TMZ–anthranilic acid cocrystal (2:1) shows a broad exotherm at about 170°C, corresponding to decomposition (Figure 35)

DSC of TMZ–d,l-tartaric acid cocrystal (1:1) shows a broad exotherm at about 170°C, corresponding to decomposition (Figure 36)

e) Single crystal X-ray diffraction

Good quality single crystal obtained from the crystallization solvent(s) given in Table 1 were mounted on the goniometer of Bruker SMART CCD diffractometer equipped with Mo-Kα radiation (λ = 0.71073 Å) source. Data collection (Bruker SMART), cell refinement: (Bruker SMART), data reduction (Bruker SAINT) program(s) distributed by Bruker AXS Inc. were used to solve the crystal structure. Structure refinement was carried out using SHELXS97 (G. M. Sheldrick, 1990; G. M. Sheldrick, 1997) program(s). Molecular graphics was plotted in Bruker SHELXTL, software to prepare material for publication. Crystal structure refinements were done using F^2 intensity of ALL the reflections. The weighted R-factor wR and goodness of fit S are based on F^2, conventional R-factors R are based on F, with F set to zero for negative F^2. The threshold expression of $F^2 > 2\text{sigma}(F^2)$ is used only for calculating R-factors(gt) etc. and is not relevant to the choice of reflections for refinement. R-factors based on F^2 are statistically

about twice as large as those based on F, and R-factors based on ALL data will be even larger. The thermal ellipsoid plots (ORTEP) were drawn at 35% probability of electron density for the heavy atoms. Crystallographic data are summarized in Table 5. All esds were estimated using the full covariance matrix. The cell esds are taken into account individually in the estimation of esds for distances, angles and torsion angles; correlations between esds in cell parameters are only used when they are defined by crystal symmetry. An approximate (isotropic) treatment of cell esds is used for estimating esds involving l.s. planes. The geometric parameters of hydrogen bonds in cocrystal structures are listed in Table 6.

The chemical diagram and stoichiometry of cocrystals analyzed by X-ray crystallography is given in Scheme II.

The ORTEP of TMZ–oxalic acid cocrystal shows 1:0.5 stoichiometry and the molecular components are connected through N–H···O and O–H···O hydrogen bonds between the carboxamide and carboxylic acid groups (Figure 37).

The ORTEP of TMZ–succinic acid cocrystal shows 1:0.5 stoichiometry and the molecular components are connected through N–H···O and O–H···O hydrogen bonds between the carboxamide and carboxylic acid groups (Figure 38).

The ORTEP of TMZ–salicylic acid cocrystal shows 1:1 stoichiometry and the molecular components are connected through N–H···O and O–H···O hydrogen bonds between the carboxamide and carboxylic acid groups (Figure 39).

The ORTEP of TMZ–d,l-malic acid cocrystal shows 1:0.5 stoichiometry and the molecular components are connected through N–H···O and O–H···O hydrogen bonds between the carboxamide and carboxylic acid groups (Figure 40). O6 of Malic acid has 0.5 site occupancy factor.

The ORTEP of TMZ–anthranilic acid cocrystal shows 2:1 stoichiometry and the molecular components are connected through O–H···O hydrogen bonds between carboxylic acid groups, and N–H···O and N–H···N hydrogen bonds between the amino group of anthranilic acid and Temozolomide (Figure 41). Four TMZ and two anthranilic acid molecules are shown for clarity.

The ORTEP of TMZ–d,l-tartaric acid cocrystal shows 1:1 stoichiometry and the molecular components are connected through N–H···O and O–H···O hydrogen bonds between the carboxamide and one carboxylic acid group and via O–H···N hydrogen bond

between the second carboxylic acid and tetrazinone ring N atom (Figure 42).

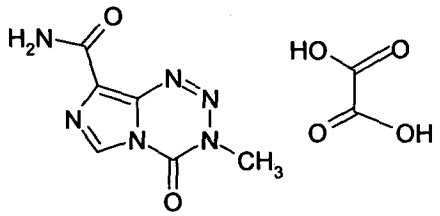

TMZ-Oxalic acid (1:0.5)

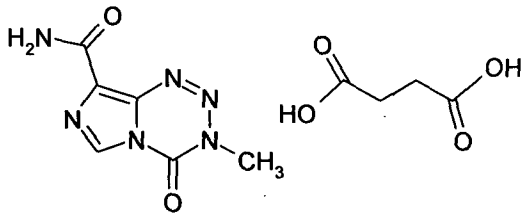

TMZ-Succinic acid (1:0.5)

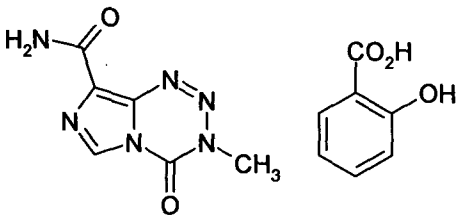

TMZ-Salicylic acid (1:1)

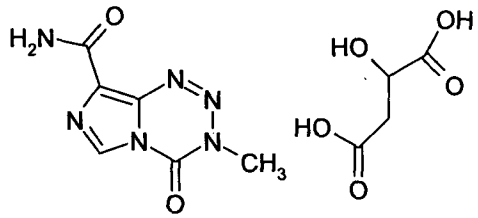

TMZ-d,l-Malic acid (1:0.5)

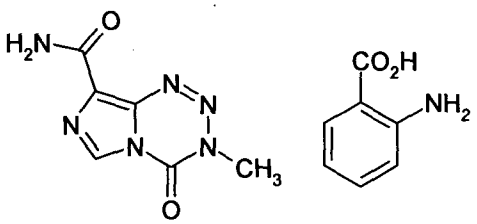

TMZ-anthranilic acid (2:1)

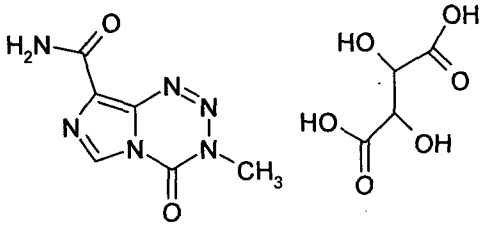

TMZ-d,l-Tartaric acid (1:1)

Scheme II: Chemical diagram and stoichiometry of Temozolomide–carboxylic acid cocrystals analyzed by single crystal X-ray diffraction.

Table 5: Crystallographic parameters for Temozolomide–carboxylic acid cocrystal structures.

	TMZ–oxalic acid (1:0.5)	TMZ–succinic acid (1:0.5)	TMZ–salicylic acid (1:1)
Empirical formula	$2(C_6H_6N_6O_2).(C2H2O4)$	$2(C_6H_6N_6O_2).(C_4H_6O_4)$	$(C_6H_6N_6O_2).(C_7H_6O_3)$
Formula weight	478.37	506.42	332.29
Crystal system	Monoclinic	Monoclinic	Triclinic
Mo-Kα λ (Å)	0.71073	0.71073	0.71073

T (K)	298(2)	100(2)	298(2)
Space group	*C*2/*c*	$P2_1/n$	$P\bar{1}$
a (Å)	14.882(2)	12.7511(13)	6.9915(14)
b (Å)	6.6222(9)	7.0092(7)	8.5449(17)
c (Å)	19.655(3)	12.9685(14)	12.682(3)
α (°)	90	90	74.003(3)
β (°)	101.156(2)	118.3580(10)	87.822(4)
γ (°)	90	90	82.328(4)
V (Å^3)	1900.4(5)	1019.97(18)	721.8(3)
D (g cm^{-3})	1.672	1.649	1.529
μ (mm^{-1})	0.140	0.135	0.121
θ range	2.79 to 25.97	3.41 to 25.93	2.50 to 25.80
2θmax	52.08	52.10	52.14
Z	8	4	2
range *h*	-18 to +18	-15 to +15	-8 to +8
range *k*	-8 to +8	-8 to +8	-10 to +10
range *l*	-24 to +24	-16 to +16	-15 to +15
F (000)	984	524	344
reflections collected	6714	10137	4408
observed reflections	1873	2016	2838
total reflections	1383	1735	1697
No. of parameters	167	176	234
R_1 [$I > 2\ \sigma(I)$]	0.0532	0.0512	0.0592
wR_2 (all)	0.1453	0.1161	0.1480
goodness-of-fit	1.07	1.09	0.98

	TMZ–d, l-malic acid (1:0.5)	TMZ–anthranilic acid (2:1)	TMZ–d, l-tartaric acid (1:1)
Empirical formula	$2(C_6H_6N_6O_2)$.	$2(C_6H_6N_6O_2)$,	$(C_6H_6N_6O_2)$,

	($C_4H_5O_5$)	($C_7H_7NO_2$)	($C_4H_6O_6$)
Formula weight	521.42	525.47	344.26
Crystal system	Monoclinic	Triclinic	Triclinic
Mo-Kα λ (Å)	0.71073	0.71073	0.71073
T (K)	298(2)	298(2)	298(2)
Space group	*C2/c*	$P\bar{1}$	$P\bar{1}$
a (Å)	22.597(16)	6.904(5)	7.725(2)
b (Å)	7.275(6)	10.624(7)	8.961(2)
c (Å)	13.144(10)	15.957(15)	10.791(2)
α (°)	90	87.731(9)	80.51(2)
β (°)	91.819(13)	81.223(15)	79.19(2)
γ (°)	90	78.017(11)	75.11(2)
V ($Å^3$)	2160(3)	1131.5(15)	703.7(3)
D ($g\ cm^{-3}$)	1.603	1.542	1.625
μ (mm^{-1})	0.134	0.120	0.142
θ range	3.31 to 24.69	2.34 to 26.03	2.86 to 29.13
2θmax	52.18	52.18	52.74
Z	8	2	2
range *h*	-27 to +27	-8 to +8	-9 to +9
range *k*	-8 to +8	-13 to +13	-11 to +11
range *l*	-16 to +16	-19 to +19	-13 to +13
F (000)	1076	544	356
reflections collected	5601	11776	4604
observed reflections	2080	4442	2876
total reflections	1348	3428	1861
No. of parameters	192	373	242
R_1 [$I > 2\ \sigma(I)$]	0.0907	0.0555	0.0618
wR_2 (all)	0.1677	0.1439	0.2170
goodness-of-fit	1.14	0.988	1.097

Table 6: Hydrogen bond geometrical parameters of Temozolomide–carboxylic acid cocrystal structures.

Compound	Interaction	D–H/ Å	H···A/ Å	D···A/ Å	∠D–H···A/ °	Symmetry code
TMZ–oxalic acid (1:0.5)	N1–H1A···O4	0.90	2.04	2.916(3)	165.0	1/2-x,1/2-y,1-z
	N1–H1B···N2	0.86	2.33	2.735(3)	109.0	Intramolecular
	N1–H1B···O3	0.86	2.27	3.103(2)	162.0	1/2-x,1/2-y,1-z
	O3–H3···O1	0.98	1.59	2.557(2)	166.0	1/2-x,1/2-y,1-z
	C4–H4···N6	0.93	2.41	3.335(3)	173.0	x,-1+y,z
	C6–H6A···O3	0.96	2.55	3.492(4)	168.3	x,1-y,1/2+z
TMZ–succinic acid (1:0.5)	N1–H1A···O3	0.89	2.05	2.903(3)	162.0	1/2+x,1/2-y,1/2+z
	N1–H1B···N2	0.85	2.40	2.771(3)	107.3	Intramolecular
	N1–H1B···O2	0.85	2.32	3.022(3)	139.0	1/2-x,1/2+y,3/2-z
	O4–H4A···O1	0.93	1.63	2.609(2)	171.0	-1/2+x,1/2-y,-1/2+z
	C4–H4···O1	0.95	2.59	3.118(3)	115.4	-1/2+x,1/2-y,-1/2+z
	C4–H4···N6	0.95	2.56	3.498(3)	168.3	-1/2+x,1/2-y,-1/2+z
TMZ–salicylic acid (1:1)	N1–H1A···O4	0.96	2.12	3.053(4)	163.0	x,1+y,z
	N1–H1B···N6	0.89	2.38	3.031(4)	130.0	Intramolecular
	N1–H1B···N5	0.89	2.63	3.269(4)	130.0	1-x,1-y,1-z
	O3–H3···O4	0.89	1.76	2.603(3)	158.0	Intramolecular
	O5–H5··O1	1.02	1.53	2.543(3)	169.0	x,-1+y,z
	C4–H4···O3	0.93	2.45	3.315(3)	153.7	x,1+y,-1+z
	C6–H6A···N2	0.96	2.63	3.462(4)	145.6	x,-1+y,z
	C6–H6B···O4	0.96	2.58	3.433(4)	147.4	1-x,-y,1-z
	C6–H6C···O2	0.96	2.47	3.435(4)	177.9	1-x,1-y,-z
	C10–H10···O1	0.93	2.53	3.384(4)	152.5	-x,2-y,1-z
TMZ–d,l-malic acid (1:0.5)	N1–H1A···O3	0.81	2.12	2.913(5)	169.0	x,-y,-1/2+z
	N1–H1B···N2	0.90	2.35	2.759(6)	108.0	Intramolecular
	N1–H1B···O2	0.90	2.25	3.018(5)	142.0	1/2-x,-1/2+y,3/2-z
	O4–H4A···O1	0.91	1.69	2.589(5)	168.0	x,-y,1/2+z
	C4–H4···N6	0.93	2.59	3.515(6)	171.4	x,-y,1/2+z

	C6–H6B···O6	0.96	2.54	3.471(1)	163.3	1/2-x,1/2-y,1-z
	C6–H6C···O6	0.96	2.44	3.172(9)	132.6	-1/2+x,1/2+y,z
TMZ–anthranilic acid (2:1)	N1–H1A···N2	0.88	2.42	2.789(4)	106.0	Intramolecular
	N1–H1A···N2	0.88	2.38	3.114(4)	141.0	-x,1-y,1-z
	N1–H1B···O4	0.89	2.14	3.021(4)	170.0	x,-1+y,z
	N7–H7A···N6	0.96	2.45	2.798(4)	101.0	Intramolecular
	N7–H7A···N8	0.96	2.15	3.017(4)	149.0	-x,2-y,-z
	N7–H7B···O2	0.90	2.13	3.005(4)	166.0	x,y,-1+z
	N13–H13A···O3	0.86	2.16	3.002(4)	164.0	x,y,z
	N13–H13B···O7	0.90	2.02	2.684(4)	129.0	Intramolecular
	N13–H13B···N12	0.90	2.42	2.980(4)	120.6	x,y,z
	O8–H8A···O7	0.92	1.78	2.694(4)	168.7	-x,-y,-z
	C4–H4···O4	0.93	2.39	3.288(4)	160.3	-x,2-y,1-z
	C10–H10···O2	0.93	2.56	3.470(4)	163.8	-x,2-y,1-z
	C12–H12···O8	0.96	2.39	3.229(4)	144.3	1-x,1-y,1-z
	C15–H15···O8	0.93	2.38	2.723(4)	101.3	Intramolecular
TMZ–dl-tartaric acid (1:1)	N1–H1A···O3	0.81	2.47	3.144(4)	141.0	x,y,z
	N1–H1A···N2	0.81	2.46	2.825(4)	109.0	Intramolecular
	N1–H1B···O7	0.90	2.38	3.180(4)	147.0	x,y,-1+z
	N1–H1B···O3	0.90	2.39	3.047(4)	130.0	1-x,2-y,-z
	O4–H4A···N6	0.88	2.03	2.897(3)	173.0	1-x,1-y,-z
	O5–H5···O3	0.88	2.23	2.680(3)	118.0	Intramolecular
	O5–H5···O7	0.76	2.09	2.760(3)	147.0	1-x,2-y,1-z
	O6–H6···O7	0.76	2.45	2.745(3)	100.0	Intramolecular
	O6–H6···O5	0.89	1.99	2.860(3)	166.0	1-x,2-y,1-z
	O8–H8···O1	0.95	1.62	2.567(3)	169.0	x,y,1+z
	C4–H4···O6	0.93	2.56	3.209(4)	126.7	-1+x,y,z
	C4–H4···O2	0.93	2.41	3.267(4)	152.2	-x,1-y,1-z
	C9–H9···O2	0.98	2.58	3.553(4)	171.3	1+x,y,z

Example 3

Melting points of the cocrystals

Temozolomide and its novel cocrystals are decomposed when heated above 160°C. There is no sharp melting point even for pure crystals of TMZ. All cocrystals decompose similar to the drug in attempts to determine the melting point (Table 7).

Table 7: Melting points of TMZ and its cocrystals.

Compound	TMZ	TMZ–succinic acid (1:0.5)	TMZ–oxalic acid (1:0.5)	TMZ–salicylic acid (1:1)	TMZ–malic acid (1:0.5)	TMZ–anthranilic acid (2:1)	TMZ–tartaric acid (1:1)
Melting point	210°C (dec.)	165°C (dec.)	170°C (dec.)	173°C (dec.)	169°C (dec.)	171°C (dec.)	170°C (dec.)

For reference, melting point of succinic acid 184-186°C, oxalic acid 189-190°C, salicylic acid 158-161°C, d,l-malic acid 131-132°C, anthranilic acid 146-148°C and d,l-tartaric acid 200-202°C .

Generally, the cocrystal melts in-between the melting points of component cocrystal formers (more often) or below their melting points (less often) (N. Schultheiss and A. Newman, Cryst. Growth Des., 2009, 9, 2950-2967). Here both TMZ cocrystals with oxalic acid and succinic acid (1:0.5) start to decompose at 176°C and 179°C respectively which is less than the melting point of TMZ and oxalic acid or succinic acid, whereas TMZ–salicylic cocrystal (1:1) starts to decompose at 172 °C which is in between the melting point of TMZ and salicylic acid. TMZ–d,l-tartaric acid cocrystal has decomposition temperature less than that of both TMZ and d,l-tartaric acid.

Example 4

Degradation study of the cocrystal in aqueous medium and in physiological pH 7 buffer

a) Temozolomide degradation study in aqueous medium by UV-Vis spectroscopy

10 mg TMZ was taken in 10 mL doubled distilled water and absorbance of the solution was measured. The solution was finally diluted 40 times with water (pH 6.0) and absorbance was measured. The absorbance at 210 nm, 256 nm and 330 nm wavelengths

were noted. These peaks correspond to aromatic ring, carbonyl group of TMZ; π-π*, n-π* and n-σ* electronic transition. At regular intervals of 2 h, absorbance of the solution was recorded. As the time progresses, TMZ undergoes decomposition due to hydrolytic cleavage of TMZ tetrazinone ring, indicated by the decrease of absorbance at 330 nm and 210 nm. Absorbance of 256 nm peak increases as the concentration of hydrolyzed product AIC increases. Approximately after 47 h, absorbance intensity of 330 nm and 256 nm are about equal (Figure 1) indicating 50% hydrolysis of TMZ. Further decomposition continues. The 256 nm peak is shifted slightly towards higher wavelength at 266 nm. The last UV measurement was recorded after 4 d.

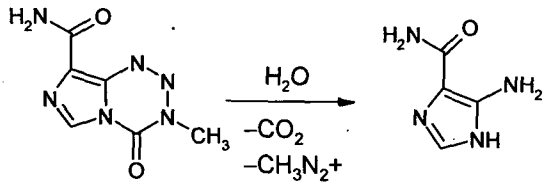

Temozolomide AIC

b) Temozolomide–Succinic acid cocrystal (1:0.5) degradation study in aqueous medium by UV-Vis spectroscopy

13 mg TMZ–Succinic acid cocrystal was taken in 10 mL doubled distilled water and absorbance of the solution was measured. The solution was diluted 40 times with water and absorbance was measured. The absorbance at 210 nm, 256 nm and 330 nm wavelengths were noted. These peaks correspond to aromatic ring, carbonyl group of TMZ; π-π*, n- π* and n-σ* electronic transitions. At regular intervals of 4 h, absorbance of the solution was recorded. As the time progresses, TMZ undergoes decomposition due to hydrolytic cleavage of TMZ tetrazinone ring, indicated by the decrease of absorbance intensity of 330 nm and 210 nm peaks. Absorbance at 256 nm increases as the concentration of hydrolyzed product AIC increases. Approximately after 86 h, absorbance of 330 nm and 256 nm are about equal (Figure 2). Further decomposition continues. The 256 nm peak is slightly shifted towards higher wavelength to 266 nm. Final UV measurements were recorded after 6 d.

c) Temozolomide–Oxalic acid cocrystal (1:0.5) degradation study in aqueous medium by UV-Vis spectroscopy

12.4 mg TMZ–oxalic acid cocrystal was taken in 10 mL doubled distilled water and absorbance of the solution was measured. The solution was diluted 40 times with water

and absorbance was measured. The absorbance at 210 nm, 256 nm and 330 nm wavelengths were noted. These peaks correspond to aromatic ring, carbonyl group of TMZ; π-π^*, n- π^* and n-σ^* electronic transitions. At regular intervals of 4 h, absorbance of the solution was recorded. As time progresses, TMZ undergoes decomposition due to hydrolytic cleavage of TMZ tetrazinone ring, indicated by the decrease of absorbance intensity of 330 nm and 210 nm peaks. Absorbance at 256 nm increases as the concentration of hydrolyzed product AIC increases. Approximately after 135 h, absorbance at 330 nm and 256 nm are about equal (Figure 3). Further decomposition continues. The 256 nm peak is shifted slightly towards higher wavelength at 266 nm. Final UV measurements were recorded after 9 d.

d) Temozolomide–Salicylic acid cocrystal (1:1) degradation study in aqueous medium by UV-Vis spectroscopy

17.1 mg TMZ–Salicylic acid cocrystal was taken in 10 mL doubled distilled water and absorbance of the solution was measured. The solution was diluted 40 times with water and absorbance was measured. The absorbance at 210 nm, 256 nm and 330 nm wavelengths were noted. These peaks correspond to aromatic ring, carbonyl group of TMZ; π-π^*, n-π^* and n-σ^* electronic transitions. In this case, salicylic acid co-former interferes with the usual observation of Temozolomide degradation because of its aromatic moiety. The absorbance at 206 nm and 296 nm peaks corresponds to π-π^*, n-π^* electronic transition. At regular intervals of 4 h, absorbance of the solution was recorded. As the time progresses, TMZ undergoes decomposition due to hydrolytic cleavage of TMZ tetrazinone ring, indicated by the decrease of absorbance at 330 nm and 210 nm. Absorbance at 256 nm increases as the concentration of hydrolyzed product increases. Approximately after 143 h, absorbance intensity of 330 nm and 256 nm peaks are equal (Figure 4). Further decomposition continues. The 256 nm peak was slightly shifted towards higher wavelength at 266 nm. Final UV measurements were recorded up to 10 d.

UV-Vis spectroscopy study showed that the half life (T½) of TMZ in distilled water at room temperature is 47 h, whereas that for cocrystals with succinic acid, oxalic acid and salicylic acid T½ increases to 86 h, 135 h and 143 h respectively under the same conditions of solvent, concentration and temperature.

e) Temozolomide degradation study in pH 7 buffer by UV-Vis spectroscopy

10 mg TMZ was taken in 10 mL pH 7 buffer and absorbance of the solution was measured. The solution was finally diluted 100 times with buffer and absorbance was measured at 37 °C. The absorbance at 210 nm, 256 nm and 330 nm wavelengths were noted. These peaks correspond to aromatic ring, carbonyl group of TMZ; π-π^*, n- π^* and n-σ^* electronic transition. At regular intervals of 15 min, absorbance of the solution was recorded. As the time progresses, TMZ undergoes decomposition due to hydrolytic cleavage of TMZ tetrazinone ring, indicated by the decrease of absorbance at 330 nm and 210 nm. Absorbance of 256 nm peak increases as the concentration of hydrolyzed product AIC increases. Approximately after 1.7 h, absorbance intensity of 330 nm and 256 nm are about equal (Figure 5) indicating 50% hydrolysis of TMZ. Further decomposition continues. The 256 nm peak is shifted slightly towards higher wavelength at 266 nm. The last UV measurement was recorded at 5.2 h. Temperature was maintained at 37 °C throughout the experiment as the condition is close to physiological pH (7.4).

f) Temozolomide-succinic acid cocrystal (1:0.5) degradation study in pH 7 buffer by UV-Vis spectroscopy

13 mg TMZ-succinic acid was taken in 10 mL pH 7 buffer and absorbance of the solution was measured. The solution was finally diluted 100 times with buffer and absorbance was measured at 37 °C. The absorbance at 210 nm, 256 nm and 330 nm wavelengths were noted. These peaks correspond to aromatic ring, carbonyl group of TMZ; π-π^*, n- π^* and n-σ^* electronic transition. At regular intervals of 15 min, absorbance of the solution was recorded. As the time progresses, TMZ undergoes decomposition due to hydrolytic cleavage of TMZ tetrazinone ring, indicated by the decrease of absorbance at 330 nm and 210 nm. Absorbance of 256 nm peak increases as the concentration of hydrolyzed product AIC increases. Approximately after 2.3 h, absorbance intensity of 330 nm and 256 nm are about equal (Figure 6) indicating 50% hydrolysis of TMZ. Further decomposition continues. The 256 nm peak is shifted slightly towards higher wavelength at 266 nm. The last UV measurement was recorded after 6 h. Temperature was maintained at 37 °C throughout the experiment.

g) Temozolomide-oxalic acid cocrystal (1:0.5) degradation study in pH 7 buffer by UV-Vis spectroscopy

12.4 mg TMZ-oxalic acid was taken in 10 mL pH 7 buffer and absorbance of the solution was measured. The solution was finally diluted 100 times with buffer and absorbance was measured at 37 °C. The absorbance at 210 nm, 256 nm and 330 nm wavelengths were noted. These peaks correspond to aromatic ring, carbonyl group of TMZ; π-π^*, n- π^* and n-σ^* electronic transition. At regular intervals of 15 min, absorbance of the solution was recorded. As the time progresses, TMZ undergoes decomposition due to hydrolytic cleavage of TMZ tetrazinone ring, indicated by the decrease of absorbance at 330 nm and 210 nm. Absorbance of 256 nm peak increases as the concentration of hydrolyzed product AIC increases. Approximately after 3.5 h, absorbance intensity of 330 nm and 256 nm are about equal (Figure 7) indicating 50% hydrolysis of TMZ. Further decomposition continues. The 256 nm peak is shifted slightly towards higher wavelength at 266 nm. The last UV measurement was recorded after 13.3 h. The temperature was maintained at 37 °C throughout the experiment.

h) Temozolomide-salicylic acid cocrystal (1:1) degradation study in pH 7 buffer by UV-Vis spectroscopy

17.1 mg TMZ-salicylic acid was taken in 10 mL pH 7 buffer and absorbance of the solution was measured. The solution was finally diluted 100 times with buffer and absorbance was measured at 37 °C. The absorbance at 210 nm, 256 nm and 330 nm wavelengths were noted. These peaks correspond to aromatic ring, carbonyl group of TMZ; π-π^*, n- π^* and n-σ^* electronic transition. At regular intervals of 15 min, absorbance of the solution was recorded. As the time progresses, TMZ undergoes decomposition due to hydrolytic cleavage of TMZ tetrazinone ring, indicated by the decrease of absorbance at 330 nm and 210 nm. Absorbance of 256 nm peak increases as the concentration of hydrolyzed product AIC increases. Approximately after 3.6 h, absorbance intensity of 330 nm and 256 nm are about equal (Figure 8) indicating 50% hydrolysis of TMZ. Further decomposition continues. The 256 nm peak is shifted slightly towards higher wavelength at 266 nm. The last UV measurement was recorded after 13.6 h. Temperature was maintained at 37 °C throughout the experiment.

i) Temozolomide-d,l-malic acid cocrystal (1:0.5) degradation study in pH 7 buffer by UV-Vis spectroscopy

13.4 mg TMZ-d,l-malic acid was taken in 10 mL pH 7 buffer and absorbance of the solution was measured. The solution was finally diluted 100 times with buffer and absorbance was measured at 37 °C. The absorbance at 210 nm, 256 nm and 330 nm wavelengths were noted. These peaks correspond to aromatic ring, carbonyl group of TMZ; π-π^*, n- π^* and n-σ^* electronic transition. At regular intervals of 15 min, absorbance of the solution was recorded. As the time progresses, TMZ undergoes decomposition due to hydrolytic cleavage of TMZ tetrazinone ring, indicated by the decrease of absorbance at 330 nm and 210 nm. Absorbance of 256 nm peak increases as the concentration of hydrolyzed product AIC increases. Approximately after 2.7 h, absorbance intensity of 330 nm and 256 nm are about equal (Figure 9) indicating 50% hydrolysis of TMZ. Further decomposition continues. The 256 nm peak is shifted slightly towards higher wavelength at 266 nm. The last UV measurement was recorded after 6.8 h. Temperature was maintained at 37 °C throughout the experiment.

j) Temozolomide-anthranilic acid cocrystal (2:1) degradation study in pH 7 buffer by UV-Vis spectroscopy

13.5 mg TMZ-anthranilic acid was taken in 10 mL pH 7 buffer and absorbance of the solution was measured. The solution was finally diluted 100 times with buffer and absorbance was measured at 37 °C. The absorbance at 210 nm, 256 nm and 330 nm wavelengths were noted. These peaks correspond to aromatic ring, carbonyl group of TMZ; π-π^*, n- π^* and n-σ^* electronic transition. At regular intervals of 15 min, absorbance of the solution was recorded. As the time progresses, TMZ undergoes decomposition due to hydrolytic cleavage of TMZ tetrazinone ring, indicated by the decrease of absorbance at 330 nm and 210 nm. Absorbance of 256 nm peak increases as the concentration of hydrolyzed product AIC increases. Approximately after 2.2 h, absorbance intensity of 330 nm and 256 nm are about equal (Figure 10) indicating 50% hydrolysis of TMZ. Further decomposition continues. The 256 nm peak is shifted slightly towards higher wavelength at 266 nm. The last UV measurement was recorded after 8.8 h. Temperature was maintained at 37 °C throughout the experiment.

k) Temozolomide-d,l-tartaric acid cocrystal (1:1) degradation study in pH 7 buffer by UV-Vis spectroscopy

17.6 mg TMZ-d,l-tartaric acid was taken in 10 mL pH 7 buffer and absorbance of the solution was measured. The solution was finally diluted 100 times with buffer and absorbance was measured at 37 °C. The absorbance at 210 nm, 256 nm and 330 nm wavelengths were noted. These peaks correspond to aromatic ring, carbonyl group of TMZ; π-π^*, n- π^* and n-σ^* electronic transition. At regular intervals of 15 min, absorbance of the solution was recorded. As the time progresses, TMZ undergoes decomposition due to hydrolytic cleavage of TMZ tetrazinone ring, indicated by the decrease of absorbance at 330 nm and 210 nm. Absorbance of 256 nm peak increases as the concentration of hydrolyzed product AIC increases. Approximately after 2.5 h, absorbance intensity of 330 nm and 256 nm are about equal (Figure 11) indicating 50% hydrolysis of TMZ. Further decomposition continues. The 256 nm peak is shifted slightly towards higher wavelength at 266 nm. The last UV measurement was recorded after 6.4 h. Temperature was maintained throughout the experiment.

UV-Vis spectroscopy studies showed that the half life of Temozolomide at the human plasma concentration of 10 μM and physiological pH 7 buffer at 37 °C is 1.7 h. The half life for cocrystals of TMZ with succinic acid, oxalic acid, salicylic acid, d,l-malic acid, anthranilic acid and d,l-tartaric acid cocrystals is 2.3 h, 3.5 h, 3.6 h, 2.7 h, 2.2 h and 2.5 h respectively at the same concentration, buffer medium and temperature.

Example 5

Intrinsic dissolution of TMZ cocrystals

From the calibration curve of TMZ and its cocrystals, molar extinction coefficients (ε) were calculated. For intrinsic dissolution study, 200 mg of each sample was made into a pellet at a hydraulic pressure of 4 ton for 5 min. The pellet was compressed to provide flat surface at one end and the other end was sealed. Then the pellet was dipped in the 500 mL of pH 7 buffer solutions as the dissolution medium at 37°C with a paddle rotation speed of 150 rpm. At 5 min time interval, 5 mL of the dissolution medium was withdrawn and replaced by an equal volume of fresh medium to maintain a constant volume. Samples were filtered through 0.2 μm nylon filter and assayed for drug content UV-Vis spectrophotometrically at 210 nm. The amount of drug dissolved (mg) at each time interval was calculated for Temozolomide and TMZ cocrystals using the calibration equation and the curves are plotted in Figure 43.

The intrinsic dissolution profile and intrinsic dissolution rate for Temozolomide and its cocrystals are listed in Table 8 and 9. TMZ, TMZ-oxalic and TMZ-succinic acid cocrystals showed comparable intrinsic solubility. TMZ-salicylic acid and TMZ-malic acid showed comparable solubility profile up to 90 min, and then solubility of TMZ-malic acid increased faster than TMZ-salicylic acid. TMZ-tartaric acid showed comparable solubility with pure TMZ up to 1 h. TMZ-anthranilic acid cocrystal has lower solubility.

Table 8: Intrinsic dissolution (in mg L–1) profile (time, min) of Temozolomide and its cocrystals.

Time (min)	2	5	10	20	30	60	90	120	150
TMZ	1.588	4.301	7.770	15.378	21.442	40.474	65.708	80.839	97.720
TMZ–Oxalic acid (1:0.5)	2.088	4.187	6.739	12.671	17.907	34.704	56.798	88.001	97.545
TMZ–Succinic acid (1:0.5)	2.623	4.966	8.086	15.838	22.623	43.943	71.822	89.849	103.282
TMZ–Salicylic acid (1:1)	1.714	3.979	7.224	15.859	22.581	50.88	132.392	166.709	172.236
TMZ–d,l-Malic acid (1:0.5)	2.054	3.787	6.249	12.669	23.199	49.807	129.082	224.481	208.48
TMZ–Anthranilic acid (2:1)	0.779	1.651	3.081	6.073	10.059	21.200	36.842	68.346	90.724
TMZ–d,l-tartaric acid (1:1)	1.920	4.122	10.022	17.193	26.770	39.140	44.732	63.063	48.273

Table 9: Intrinsic dissolution rate of Temozolomide and its cocrystals.

API	TMZ	TMZ-	TMZ-	TMZ-	TMZ-	TMZ-	TMZ-

		oxalic acid (1:0.5)	succinic acid (1:0.5)	salicylic acid (1:1)	malic acid (1:0.5)	anthranilic acid (2:1)	tartaric acid (1:1)
Intrinsic dissolution rate (mg cm–2 min–1)	0.756	0.742	0.835	1.069	1.124	0.378	0.784

The results described herein above, show improved stability as well as dissolution rate of the pure drug Temozolomide imparted by combining the anti tumor drug with the said co-crystal formers which act not only as co-crystal formers but also contribute to enhance the efficacy of the anti tumor drug by their formation of the co-crystals with the parent molecule (API).

It will be evident to those skilled in the art that the invention is not limited to the details of the foregoing illustrative examples and that the present invention may be embodied in other specific forms without departing from the essential attributes thereof, and it is therefore desired that the present embodiments and examples be considered in all respects as illustrative and not restrictive, reference being made to the appended claims, rather than to the foregoing description, and all changes which come within the meaning and range of equivalency of the claims are therefore intended to be embraced therein.

We Claim,

1. Novel pharmaceutical cocrystals of temozolomide with co-crystal formers selected from aliphatic and aromatic carboxylic acids in fixed stoichiometric ratio with improved hydrolytic stability.
2. The novel pharmaceutical cocrystals of temozolomide as claimed in claim 1, wherein the aliphatic and aromatic carboxylic acids are selected from mono and dicarboxylic acids such as formic acid, acetic acid, oxalic acid, citric acid, succinic acid, salicylic acid, d,l-malic acid, d,l-tartaric acid, maleic acid, fumaric acid, cinnamic acid, malonic acid, benzoic acid, crotonic acid, p-hydroxybenzoic acid, p-aminobenzoic acid, propanoic acid, sorbic acid, linoleic acid, adipic acid, lactic acid , glutaric acid, aconitic acid, anthranilic acid, etc.
3. The novel cocrystals of temozolomide as claimed in claim 2, wherein the carboxylic acids having pKa value in the range of 2 to 6 are used as pH adjusters in cocrystals.
4. The novel pharmaceutical cocrystal of temozolomide as claimed in claim 2, is a cocrystal of temozolomide and oxalic acid (1:0.5).
5. The pharmaceutical cocrystal of temozolomide and oxalic acid as claimed in claim 4, having characteristic peaks in a powder X-ray diffraction pattern at 9.22, 14.76, 15.79, 18.01, 22.73 and 27.82 ±0.2° degrees 2 theta angle.
6. The pharmaceutical cocrystal of temozolomide and oxalic acid as claimed in claim 4, exhibit characteristic DSC exotherm at 176 °C.
7. The novel pharmaceutical cocrystal of temozolomide as claimed in claim 2, is a cocrystal of temozolomide and succinic acid (1:0.5).
8. The pharmaceutical cocrystal of temozolomide and succinic acid as claimed in claim 7 having characteristic peaks in powder X-ray diffraction pattern at 8.03, 15.71, 16.08, 26.13 and 36.27 ±0.2° degrees 2 theta angle.
9. The pharmaceutical cocrystal of temozolomide and succinic acid as claimed in claim 7, exhibit characteristic DSC exotherm at 180 °C.
10. The novel pharmaceutical cocrystal of temozolomide as claimed in claim 2, is cocrystal of temozolomide and salicylic acid (1:1).

11. The pharmaceutical cocrystal of temozolomide and salicylic acid as claimed in claim10, having characteristic peaks in powder X-ray diffraction pattern at 11.31, 14.61, 25.69, 26.65 and 28.48 ±0.2° degrees 2 theta angle.
12. The pharmaceutical cocrystal of temozolomide and salicylic acid as claimed in claim 10, exhibit characteristic DSC exotherm at 173 °C.
13. The novel pharmaceutical cocrystal of temozolomide as claimed in claim 2, is a cocrystal of temozolomide and d,l-malic acid (1:0.5).
14. The pharmaceutical cocrystal of temozolomide and d,l-malic acid as claimed in claim 13 having characteristic peaks in powder X-ray diffraction pattern at 15.93, 18.59, 20.20, 23.67, 25.82 and 26.78 ±0.2° degrees 2 theta angle.
15. The pharmaceutical cocrystal of temozolomide and d,l-malic acid as claimed in claim 13, exhibit characteristic DSC exotherm at 169 °C.
16. The novel pharmaceutical cocrystal of temozolomide as claimed in claim 2, is a cocrystal of temozolomide and anthranilic acid (2:1).
17. The pharmaceutical cocrystal of temozolomide and anthranilic acid as claimed in claim 16 having characteristic peaks in powder X-ray diffraction pattern at 11.21, 15.23, 23.43, 26.53 and 27.68 ±0.2° degrees 2 theta angle.
18. The pharmaceutical cocrystal of temozolomide and anthranilic acid as claimed in claim 16, exhibit characteristic DSC exotherm at 171 °C.
19. The novel pharmaceutical cocrystal of temozolomide as claimed in claim 2, is a cocrystal of temozolomide and d,l-tartaric acid (1:1).
20. The pharmaceutical cocrystal of temozolomide and d,l-tartaric acid as claimed in claim 19 having characteristic peaks in powder X-ray diffraction pattern at 10.34, 20.61, 24.39, 27.38 and 29.07 ±0.2° degrees 2 theta angle.
21. The pharmaceutical cocrystal of temozolomide and d,l- tartaric acid as claimed in claim 19, exhibit characteristic DSC exotherm at 170 °C.
22. The pharmaceutical cocrystal of temozolomide and oxalic acid as claimed in claim 4, having improved stability in water as measured by UV-Vis spectra and shown in Figure 3.
23. The pharmaceutical cocrystal of temozolomide and succinic acid as claimed in claim 7, having improved stability in water as measured by UV-Vis spectra and shown in Figure 2.

24. The cocrystal of temozolomide and salicylic acid as claimed in claim 10, having improved stability in water as measured by UV-Vis spectra and shown in Figure 4.
25. The cocrystal of temozolomide and oxalic acid as claimed in claim 4, having improved stability in pH 7 buffer as measured by UV-Vis spectra and shown in Figure 7.
26. The pharmaceutical cocrystal of temozolomide and succinic acid as claimed in claim 7, having improved stability in pH 7 buffer as measured by UV-Vis spectra and shown in Figure 6.
27. The cocrystal of temozolomide and salicylic acid as claimed in claim 10, having improved stability in pH 7 buffer as measured by UV-Vis spectra and shown in Figure 8.
28. The cocrystal of temozolomide and d,l-malic acid as claimed in claim 13, having improved stability in pH 7 buffer as measured by UV-Vis spectra and shown in Figure 9.
29. The pharmaceutical cocrystal of temozolomide and anthranilic acid as claimed in claim 15, having improved stability in pH 7 buffer as measured by UV-Vis spectra and shown in Figure 10.
30. The cocrystal of temozolomide and d,l-tartaric acid as claimed in claim 19, having improved stability in pH 7 buffer as measured by UV-Vis spectra and shown in Figure 11.
31. A pharmaceutical composition comprising a novel temozolomide–oxalic acid (1:0.5) cocrystal as claimed in claim 4 in association with one or more pharmaceutically acceptable carriers.
32. A pharmaceutical composition comprising a novel temozolomide–succinic acid (1:0.5) cocrystal as claimed in claim 7 in association with one or more pharmaceutically acceptable carriers.
33. A pharmaceutical composition comprising a novel temozolomide–salicylic acid (1:1) cocrystal as claimed in claim 10, in association with one or more pharmaceutically acceptable carriers.
34. A pharmaceutical composition comprising a novel temozolomide–d,l-malic acid (1:0.5) cocrystal as claimed in claim 13 in association with one or more pharmaceutically acceptable carriers.

35. A pharmaceutical composition comprising a novel temozolomide–anthranilic acid (2:1) cocrystal as claimed in claim 16 in association with one or more pharmaceutically acceptable carriers.
36. A pharmaceutical composition comprising a novel temozolomide–d,l-tartaric acid (1:1) cocrystal as claimed in claim 19, in association with one or more pharmaceutically acceptable carriers.
37. Temozlomide cocrystals as claimed in claim 2 and of Intrinsic Dissolution Rate as listed in Table 9.

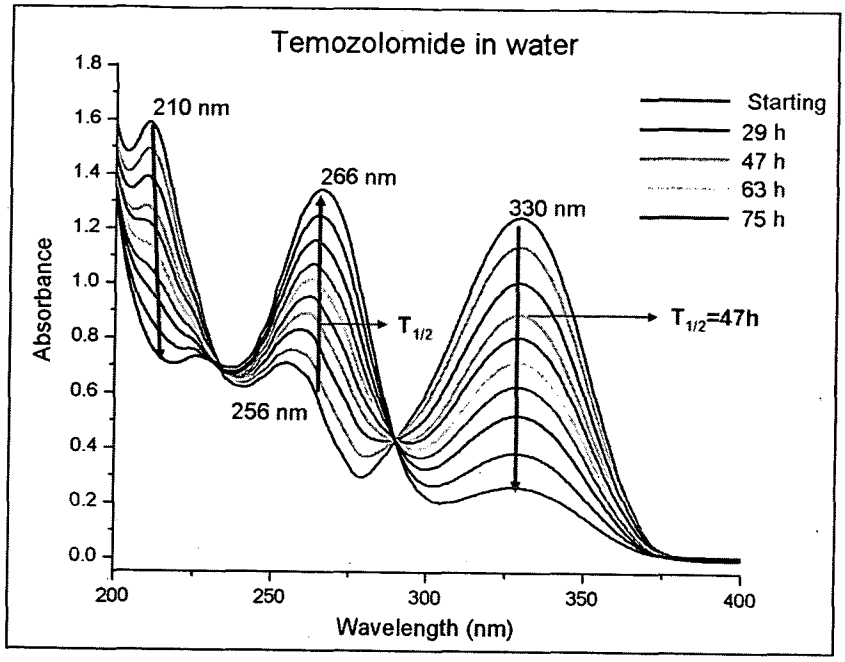

Figure 1

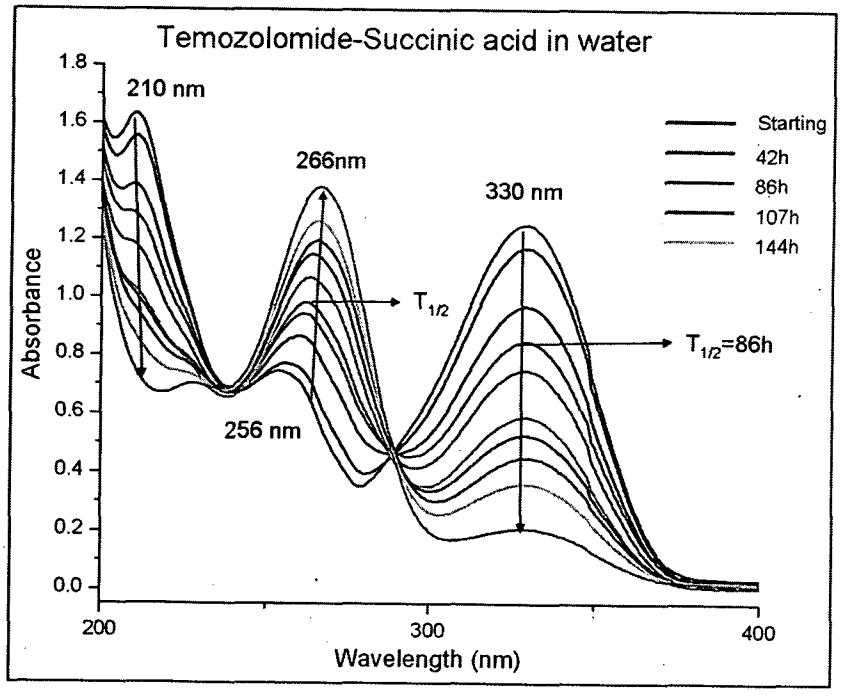

Figure 2

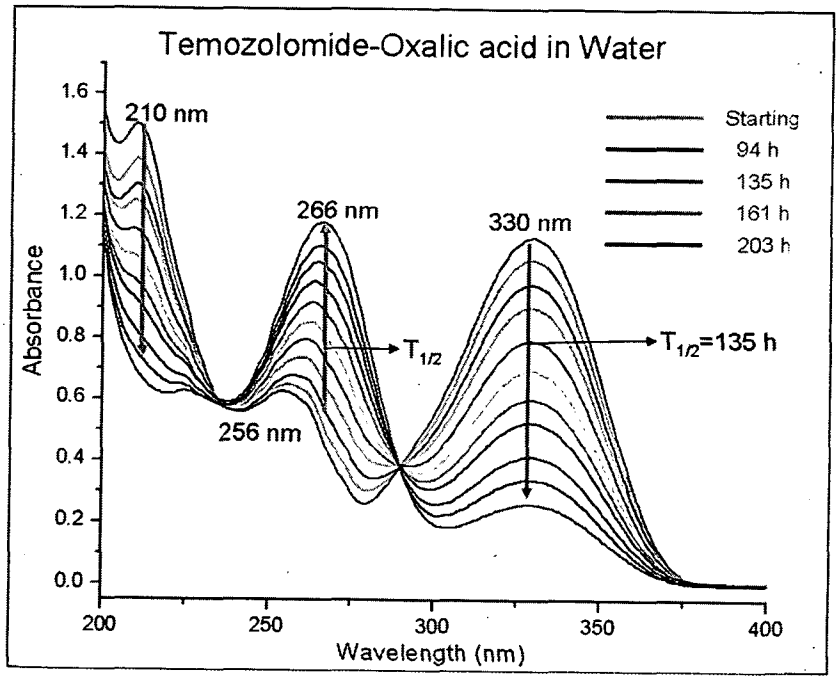

Figure 3

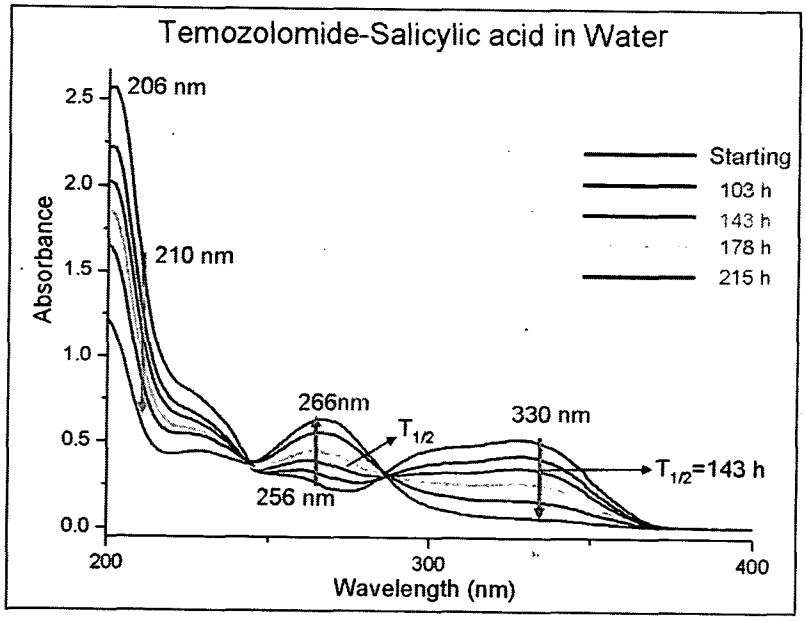

Figure 4

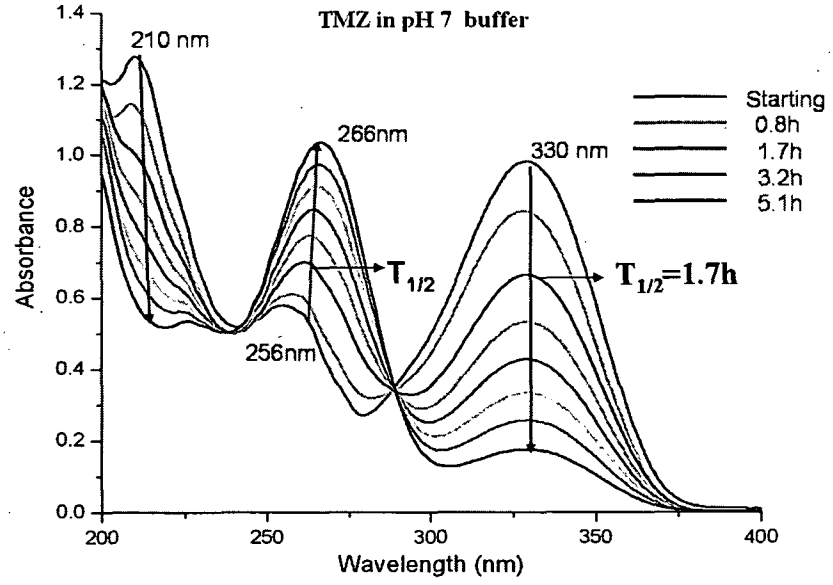

Figure 5

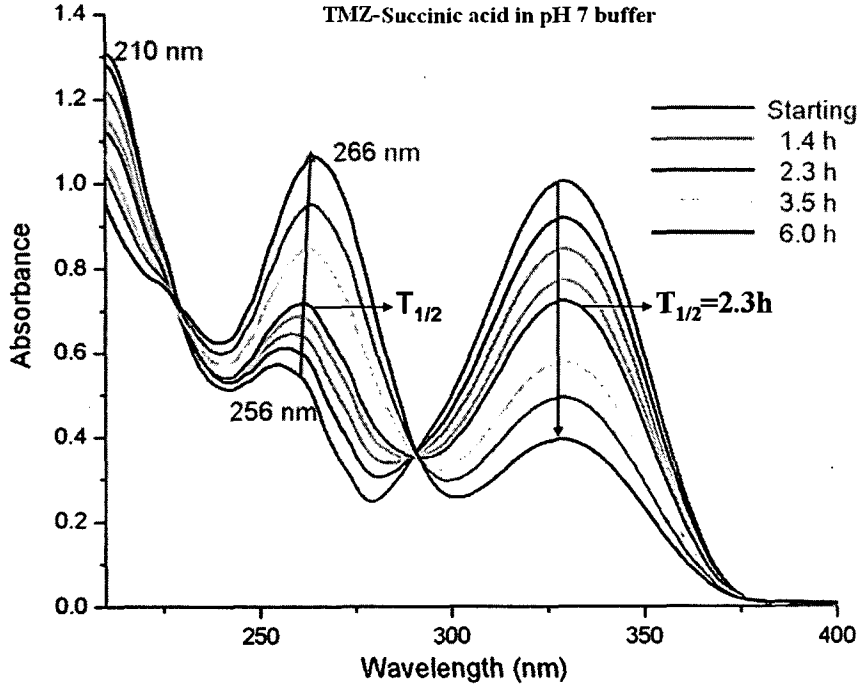

Figure 6

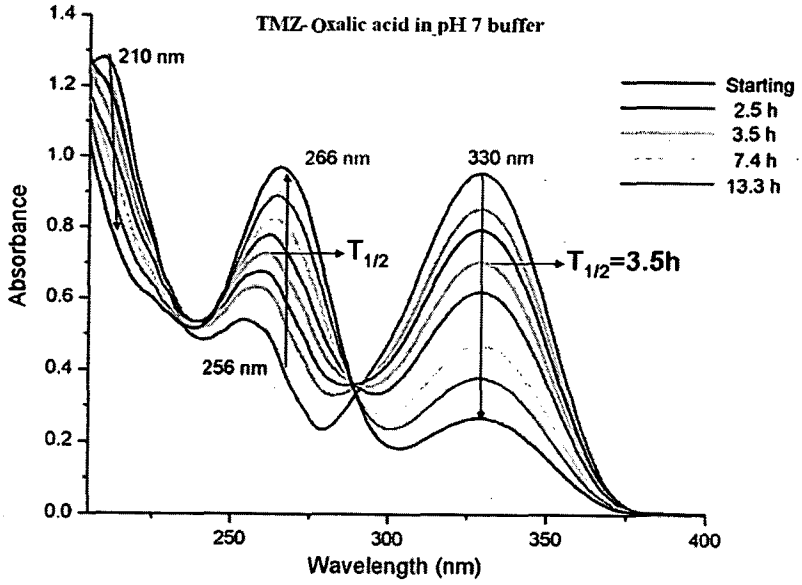

Figure 7

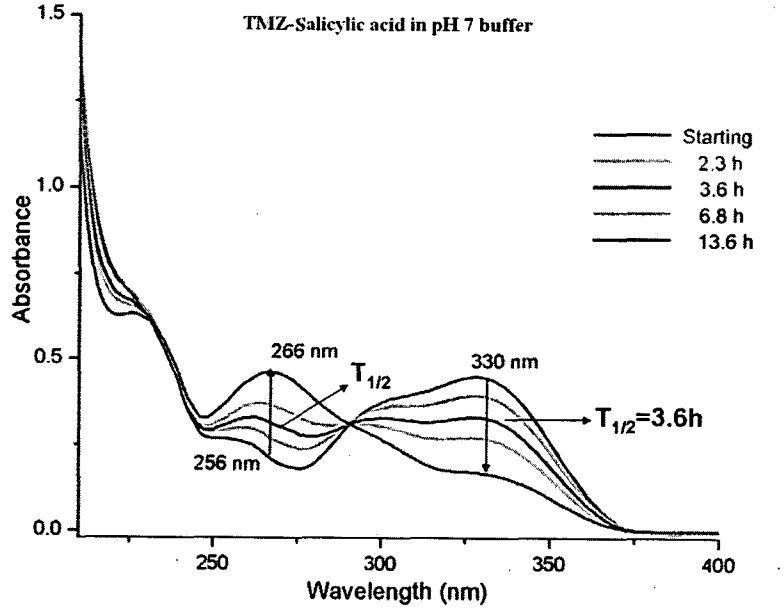

Figure 8

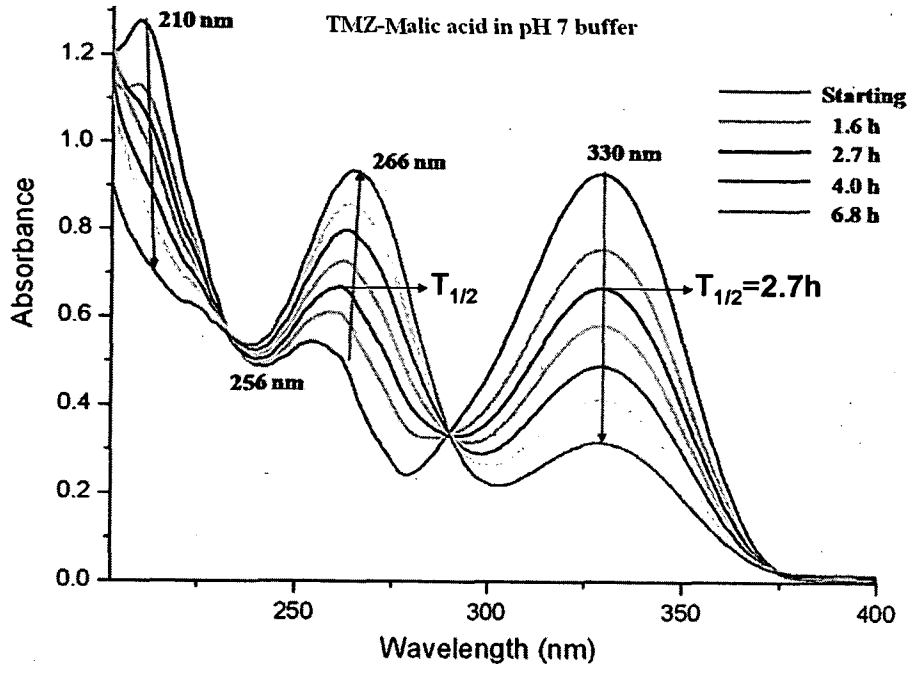

Figure 9

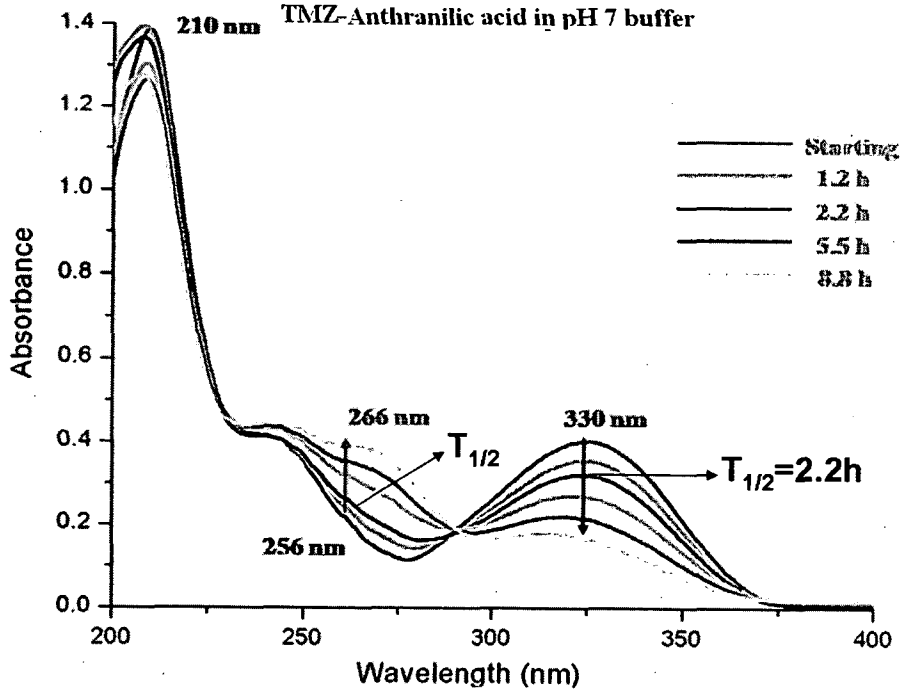

Figure 10

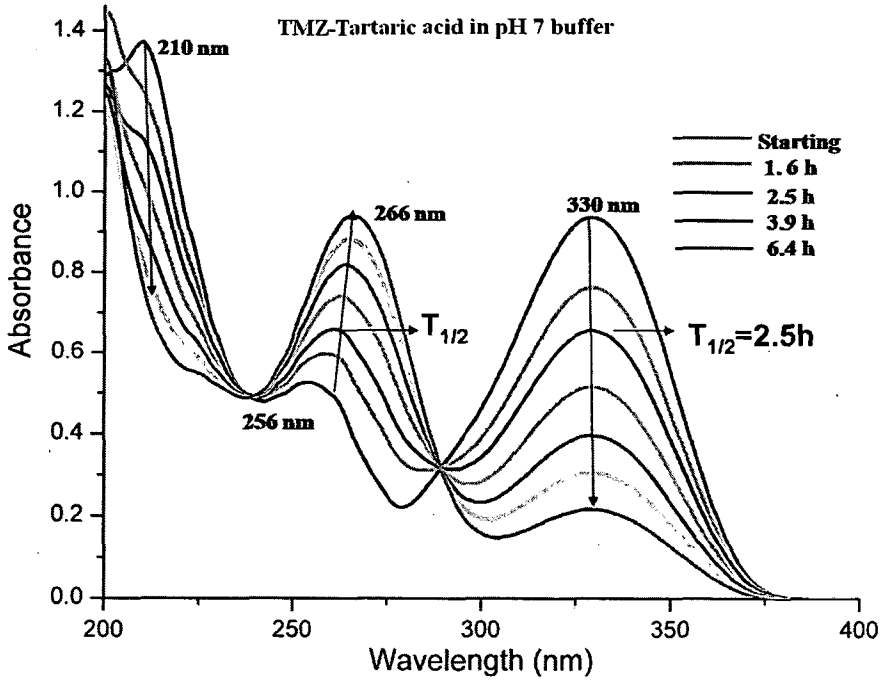

Figure 11

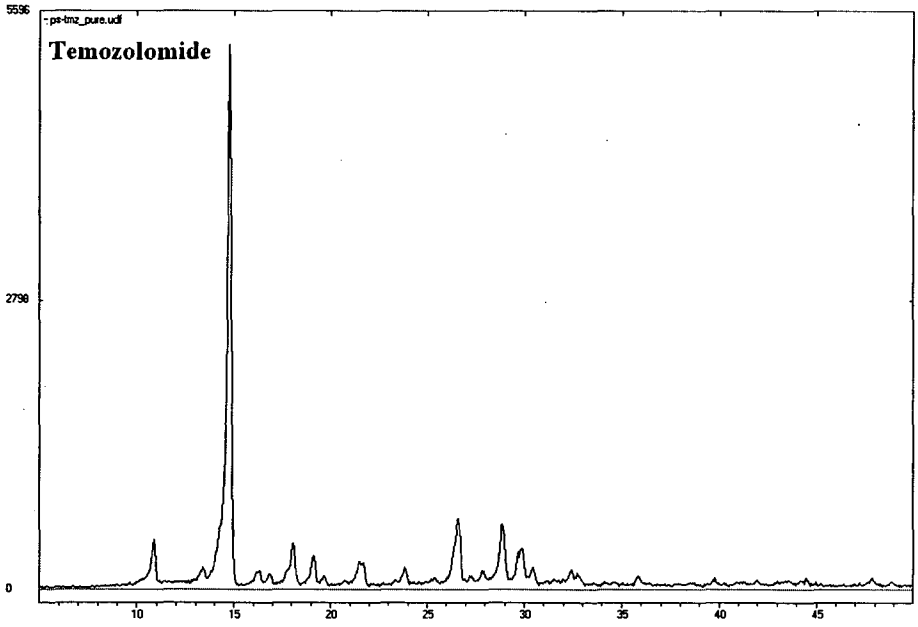

Figure 12

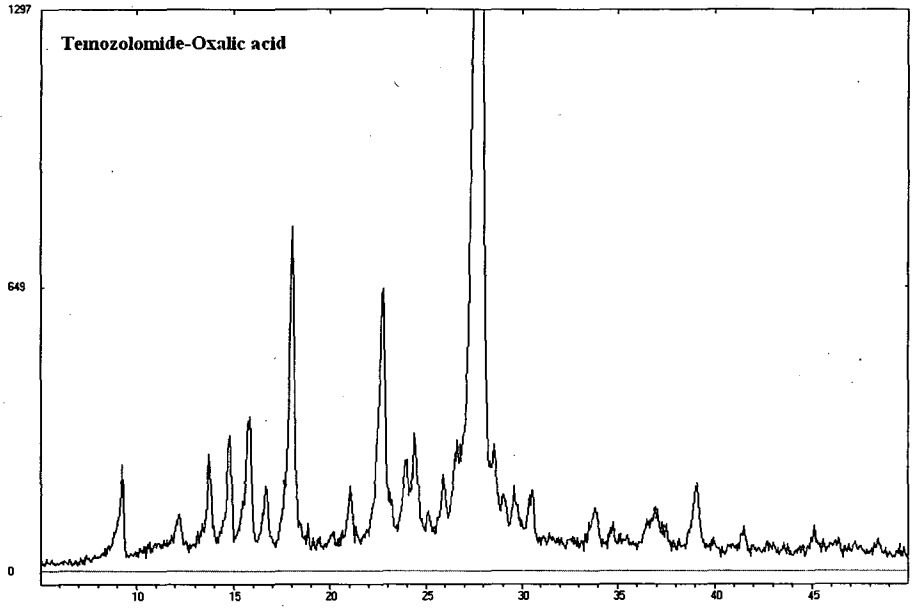

Figure 13

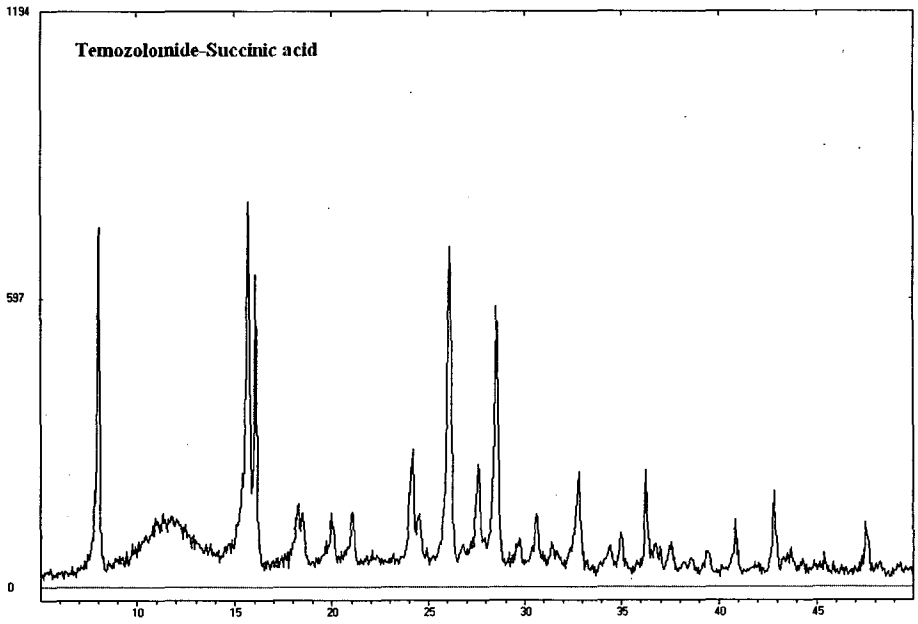

Figure 14

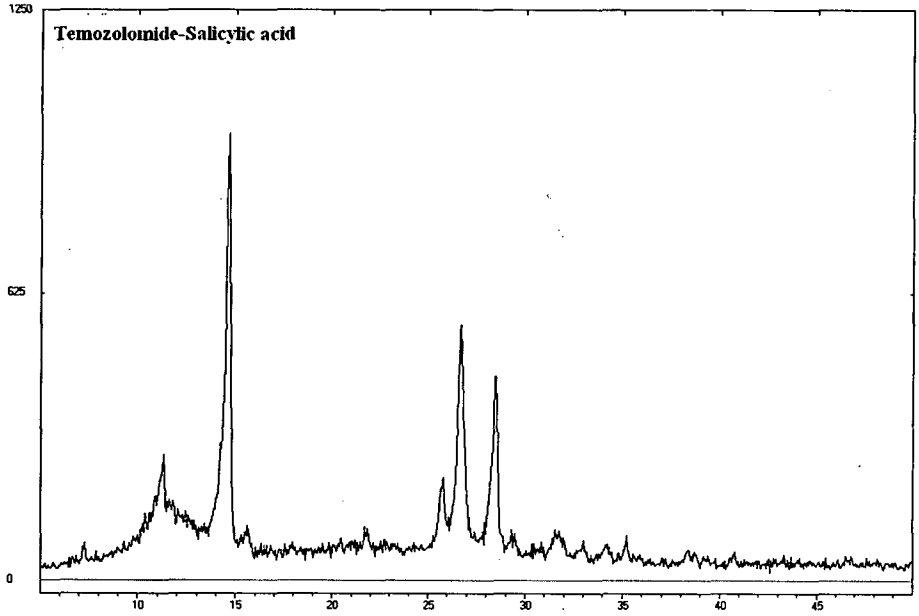

Figure 15

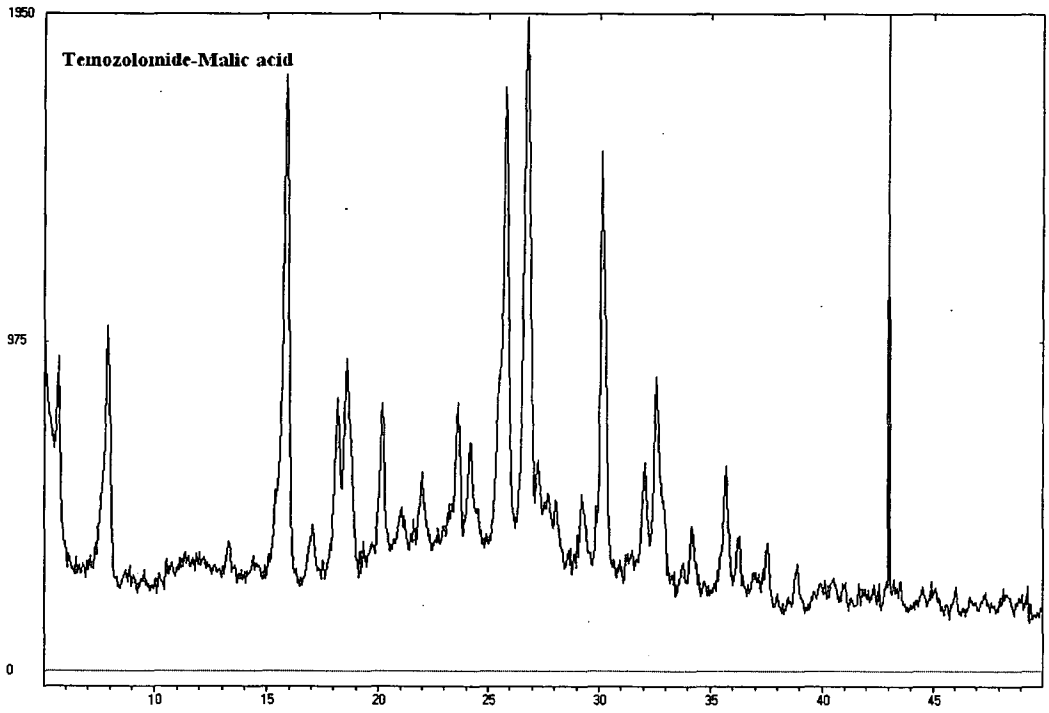

Figure 16

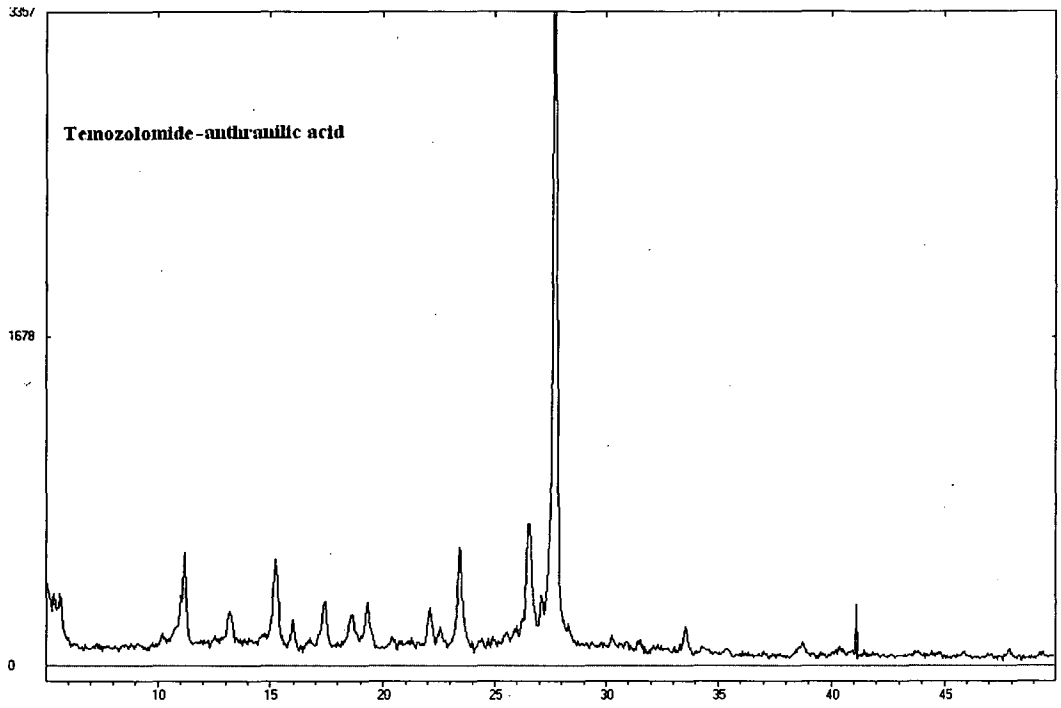

Figure 17

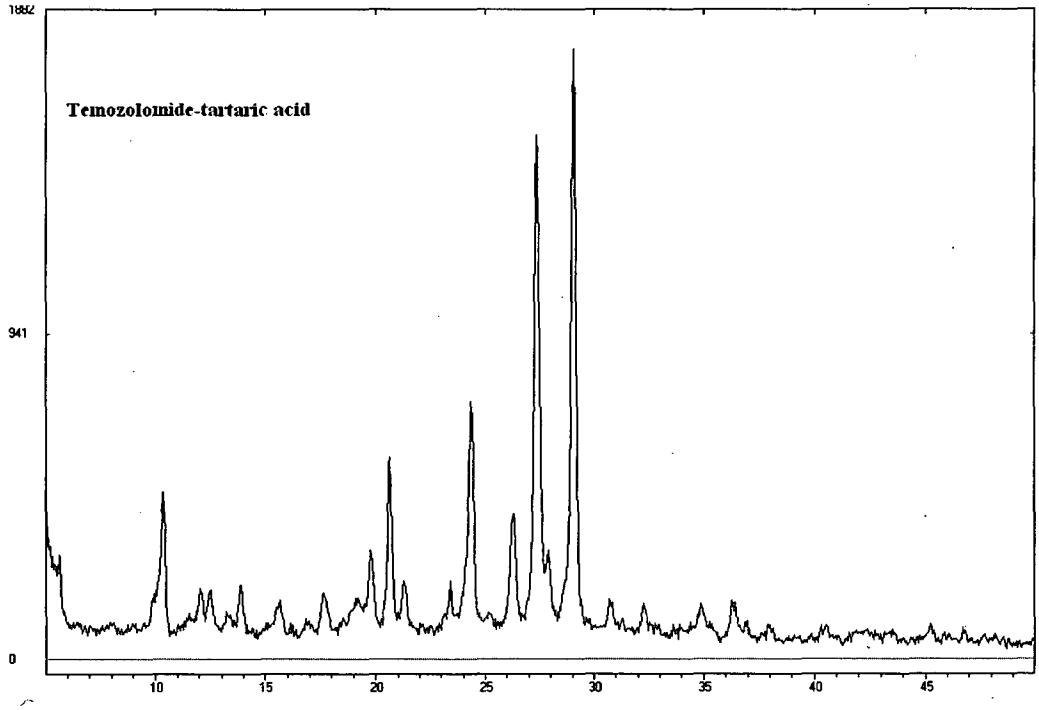

Figure 18

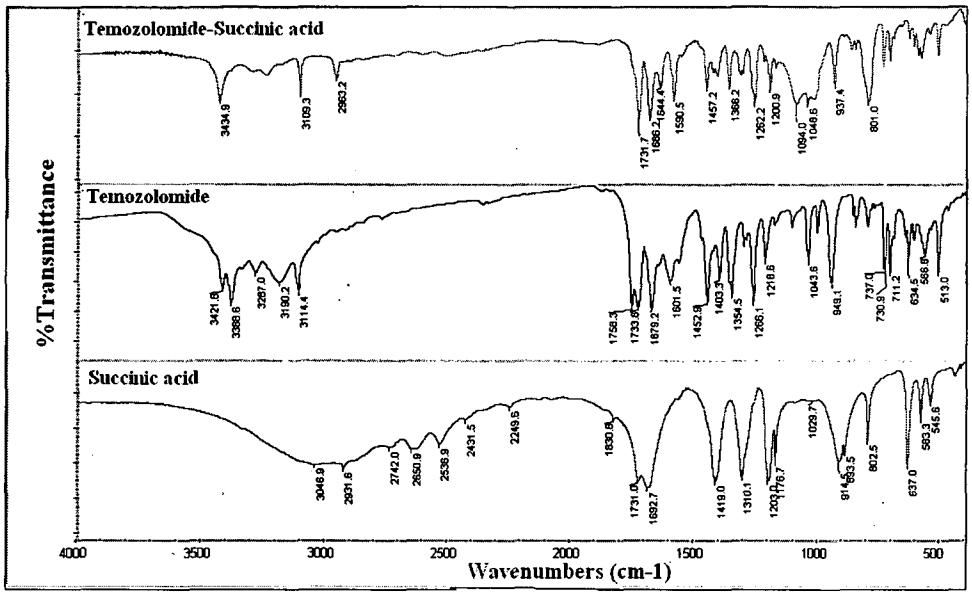

Figure 19

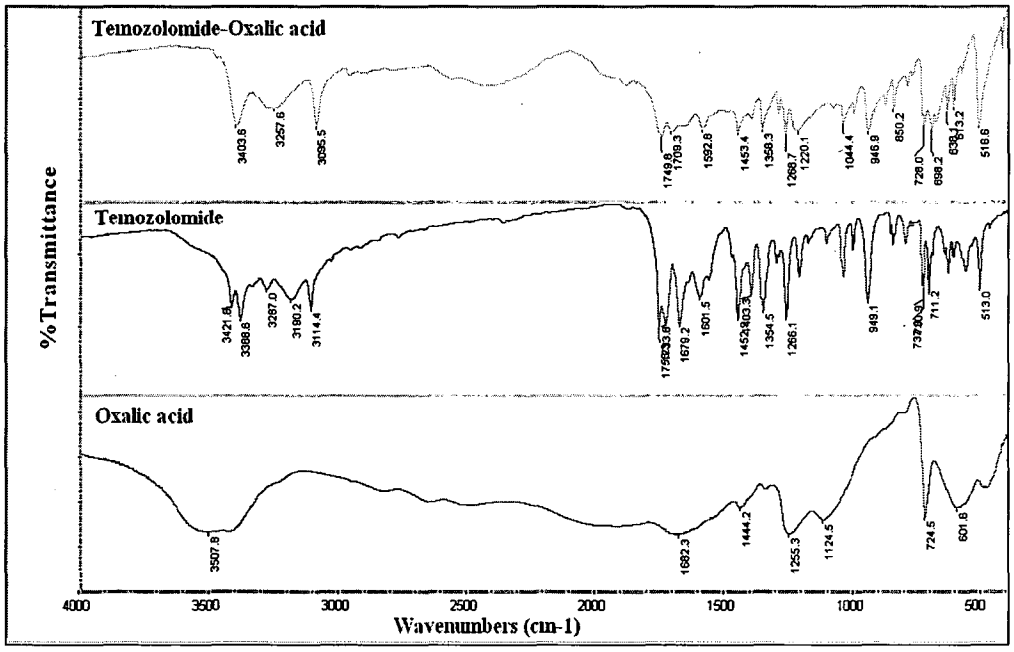

Figure 20

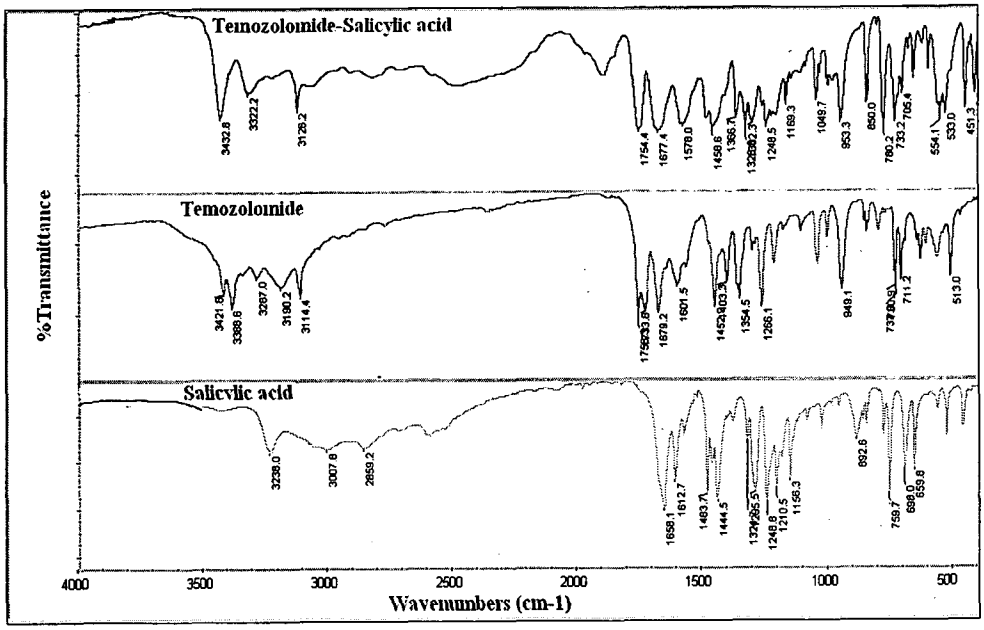

Figure 21

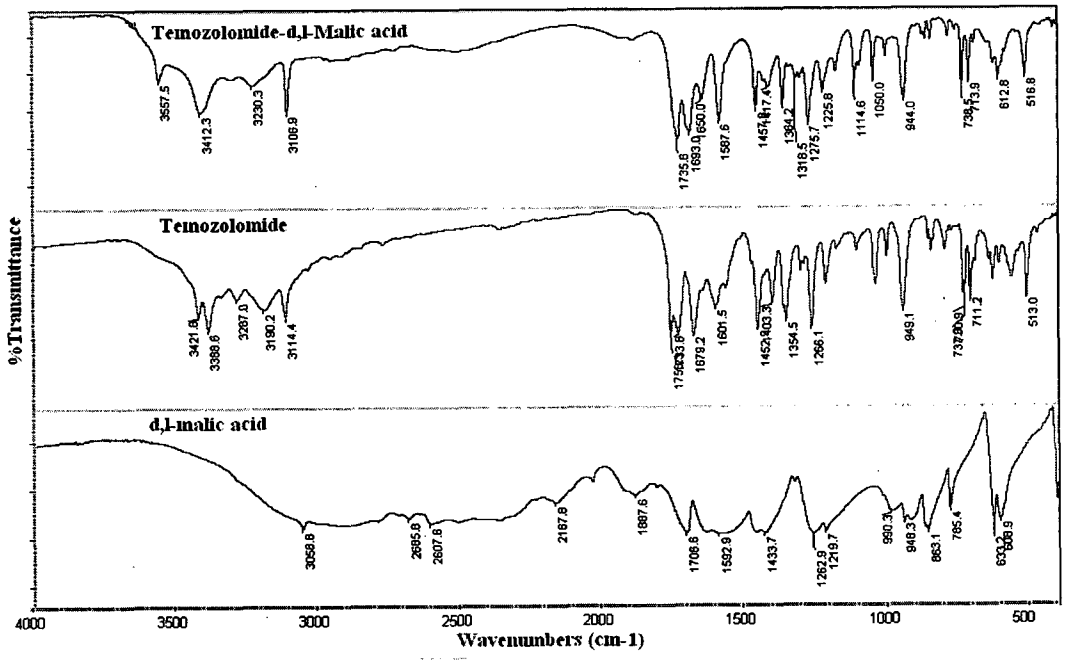

Figure 22

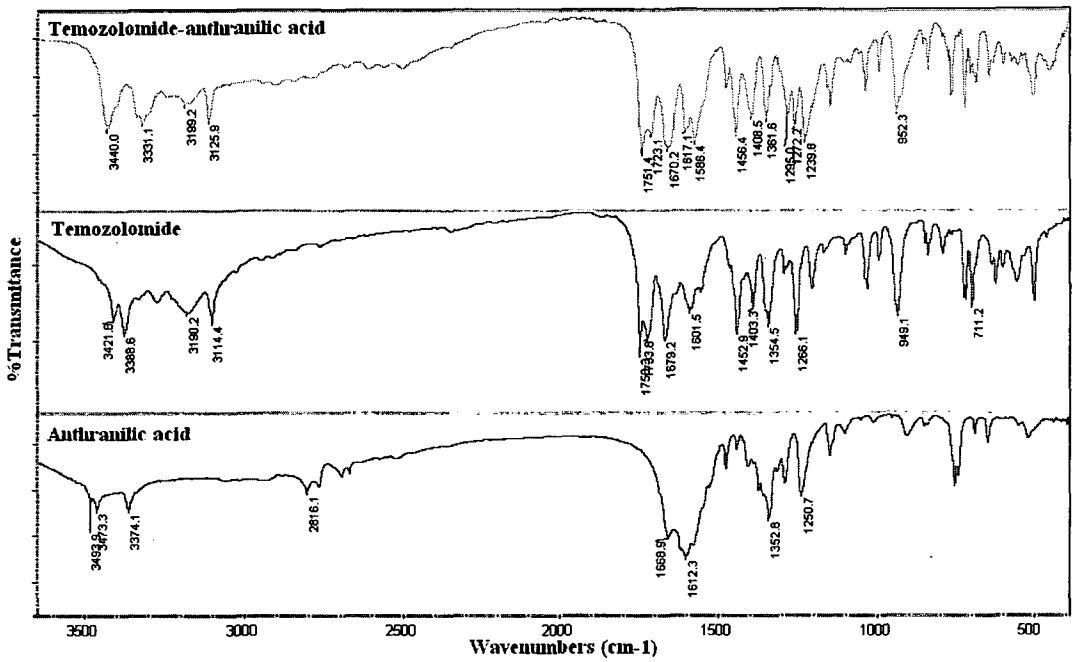

Figure 23

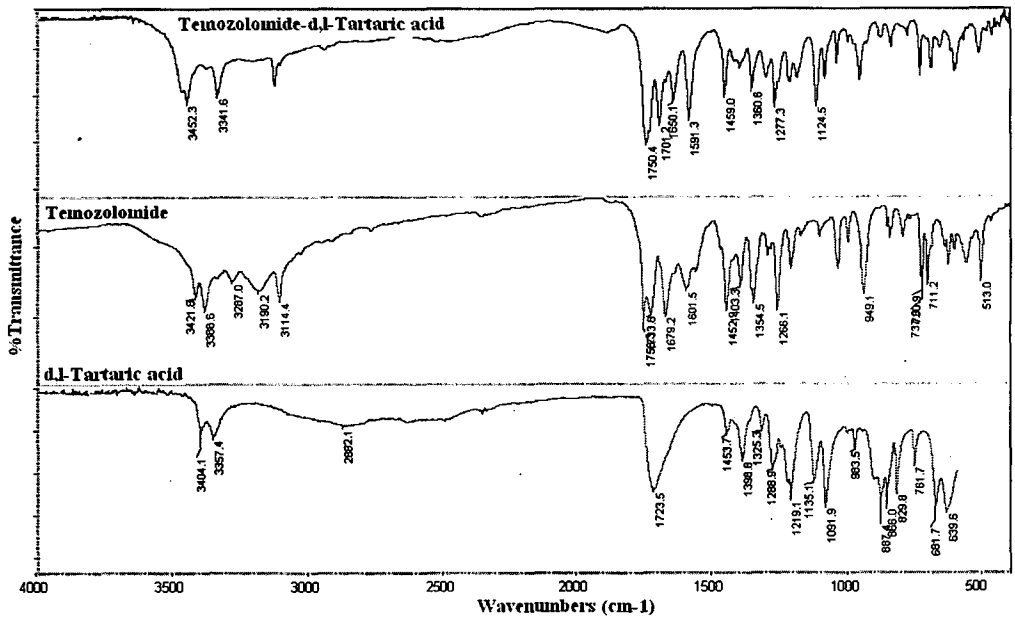

Figure 24

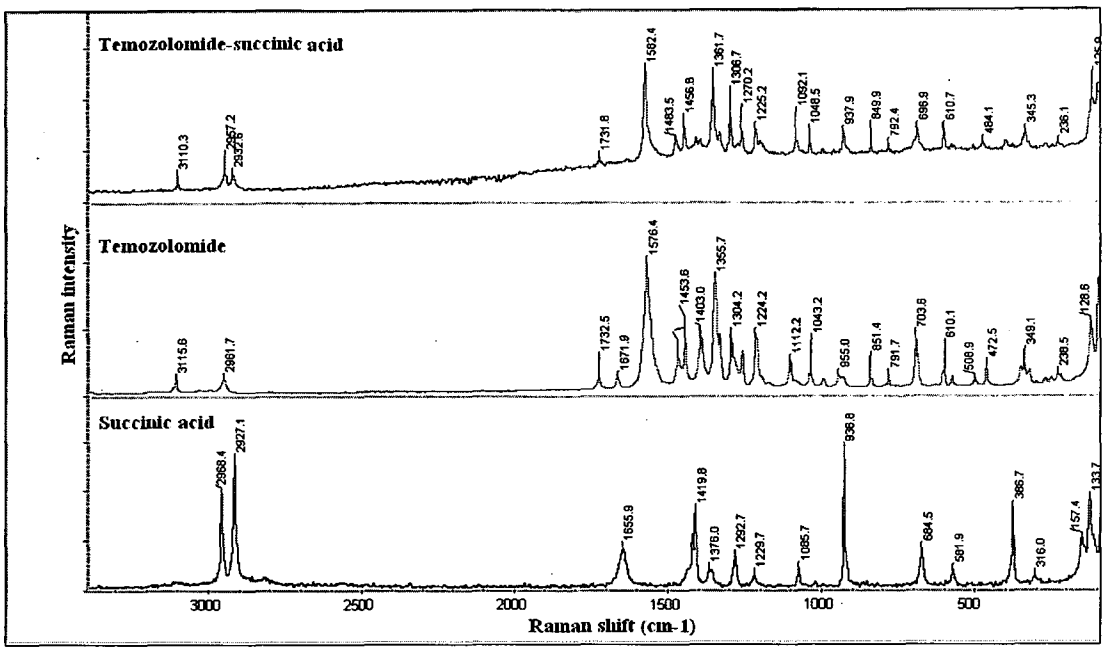

Figure 25

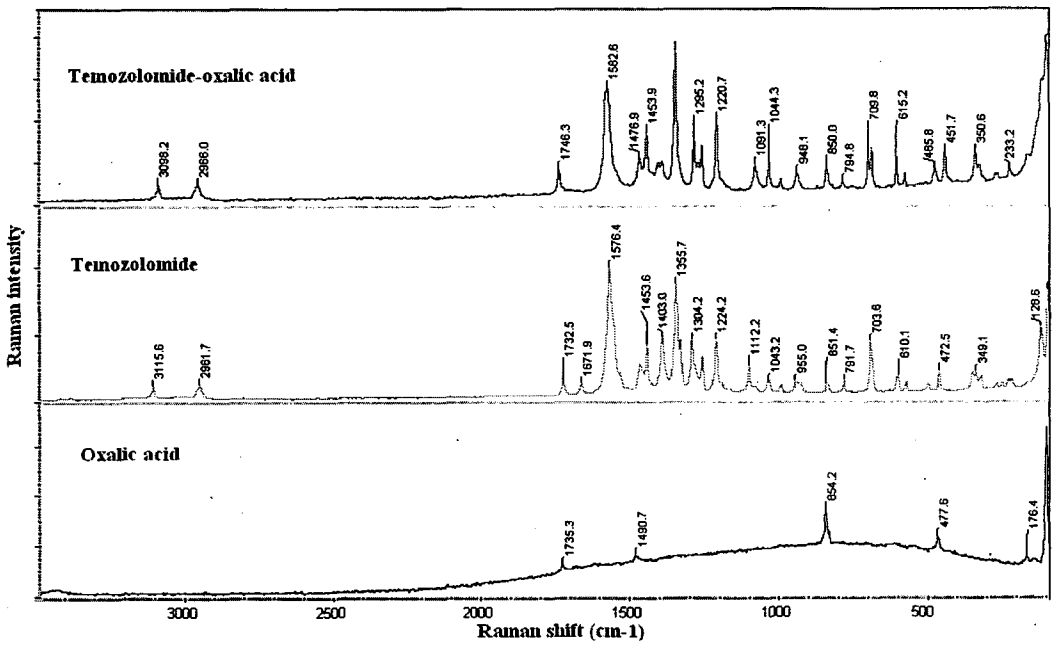

Figure 26

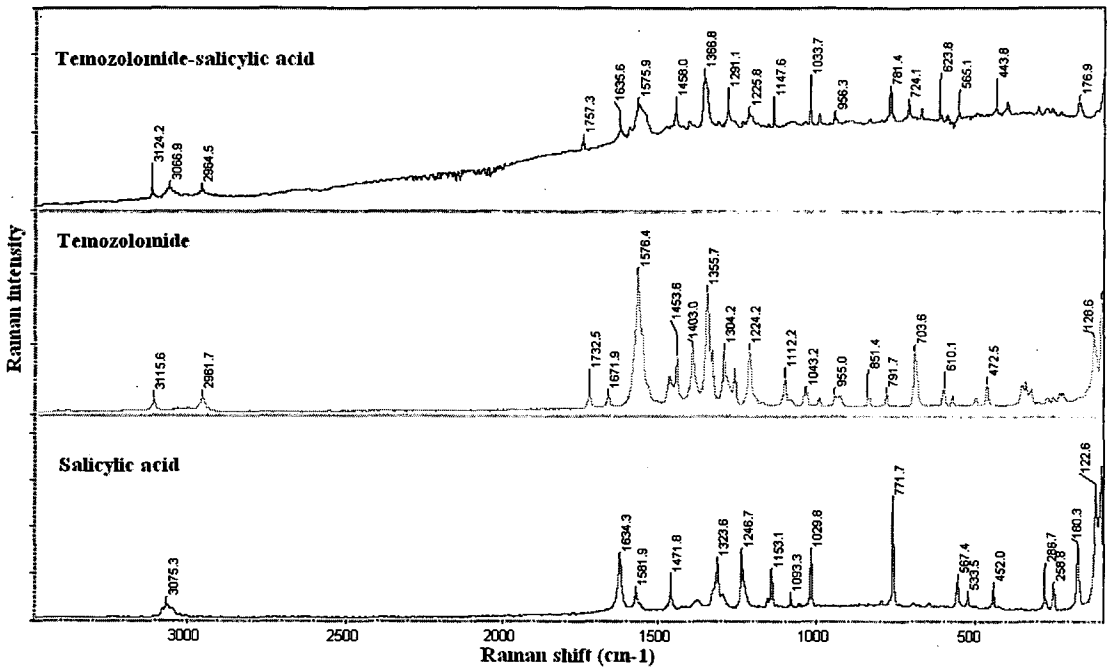

Figure 27

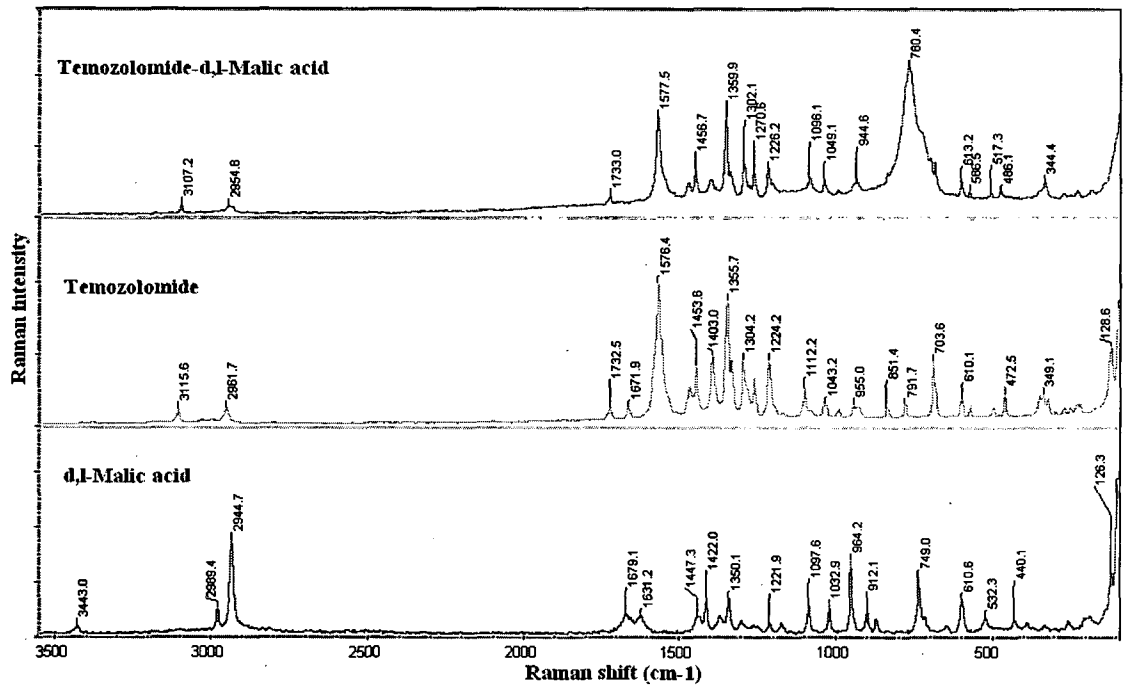

Figure 28

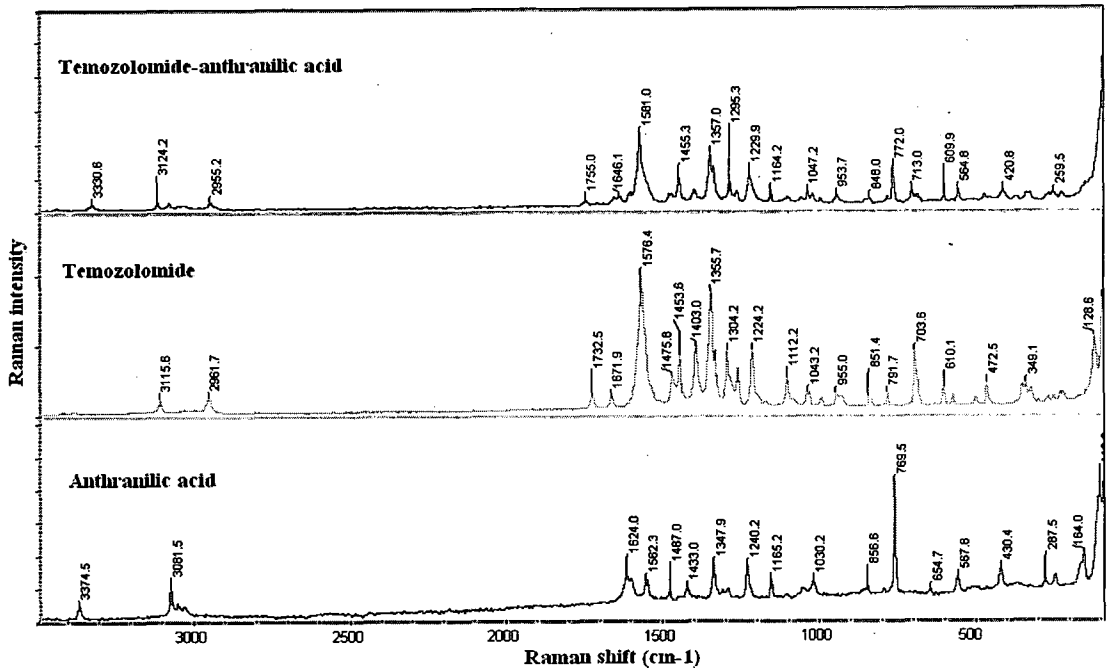

Figure 29

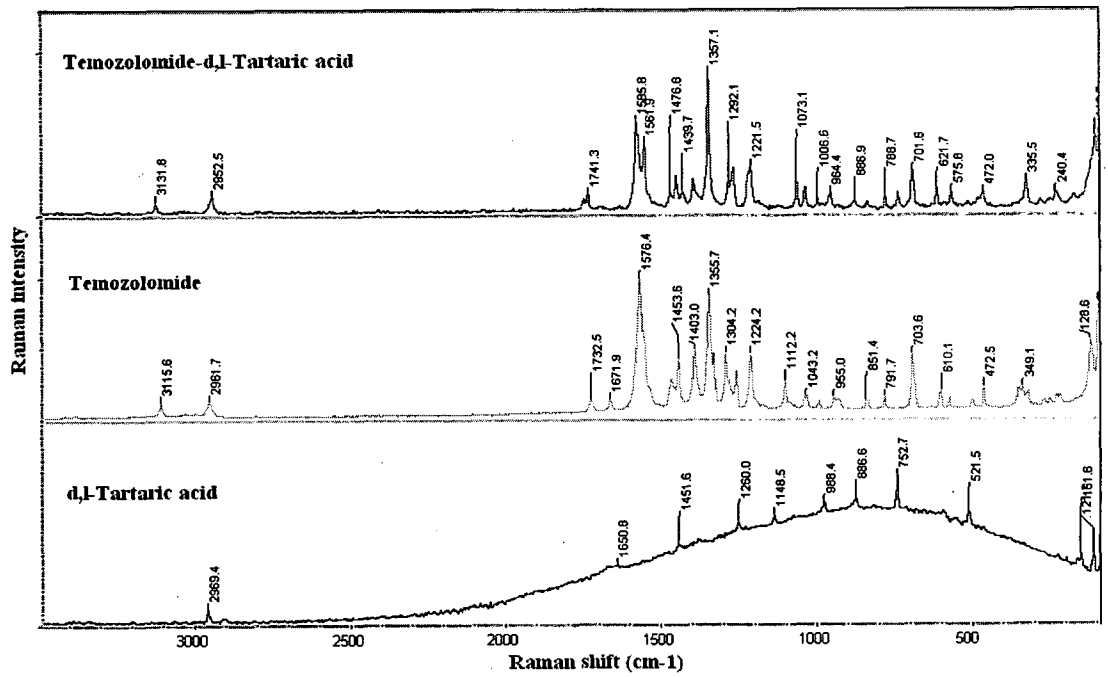

Figure 30

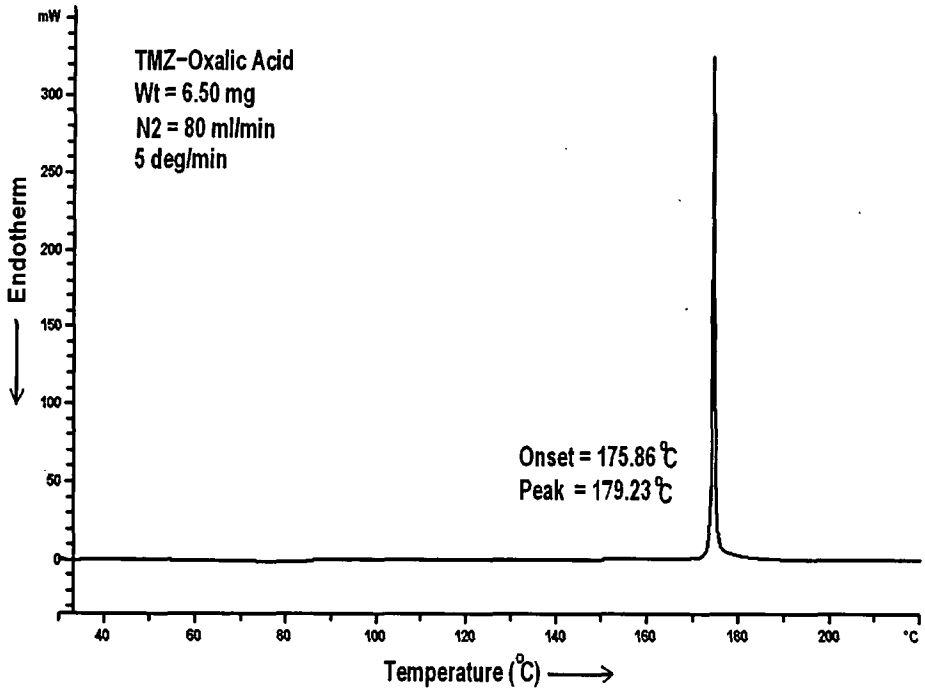

Figure 31

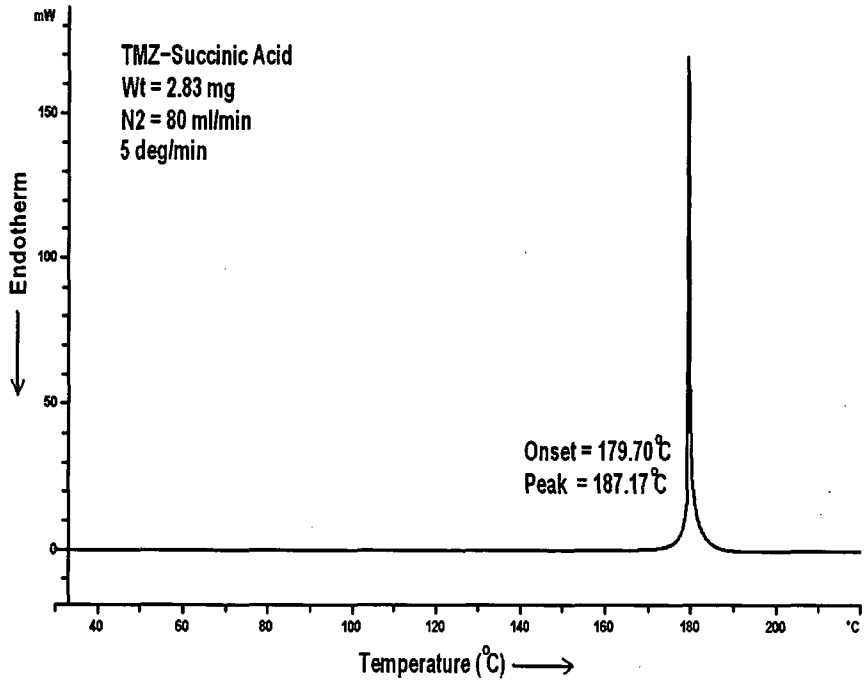

Figure 32

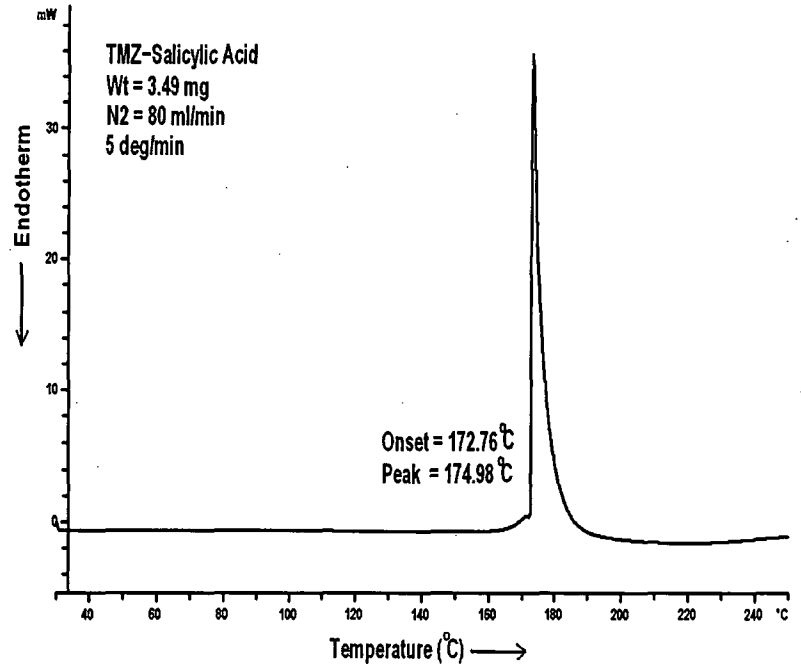

Figure 33

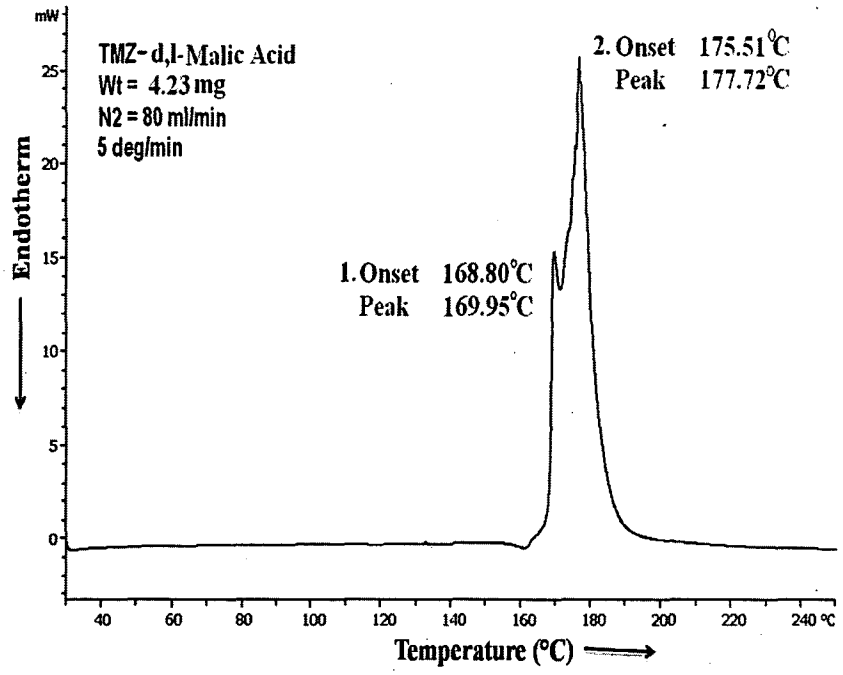

Figure 34

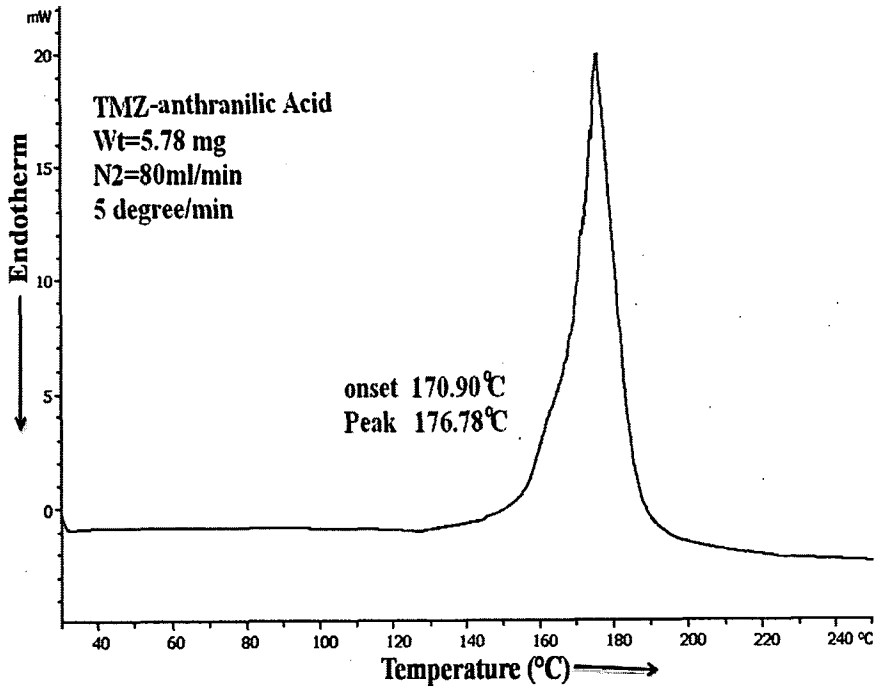

Figure 35

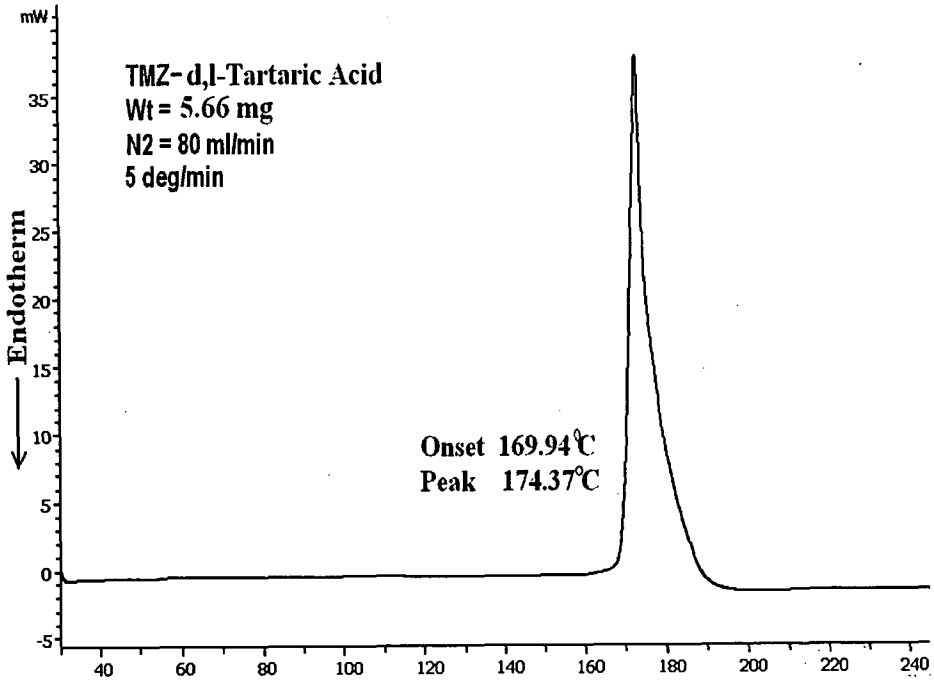

Figure 36

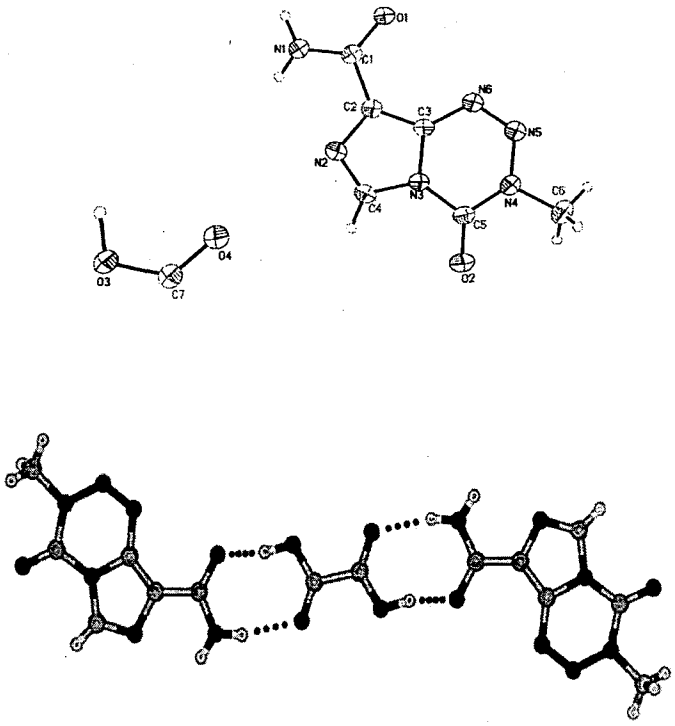

Figure 37

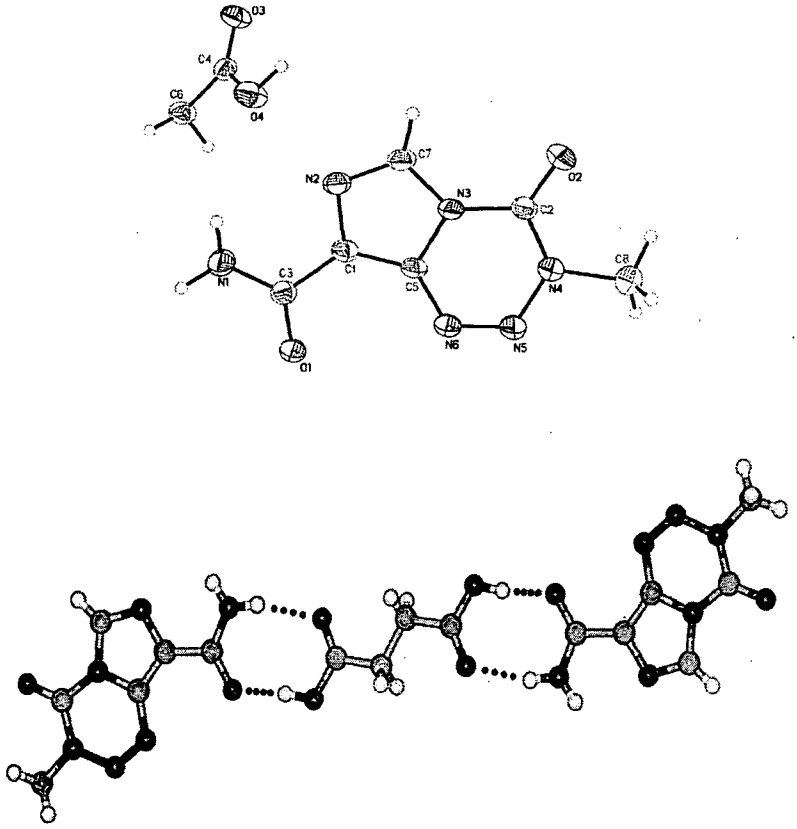

Figure 38

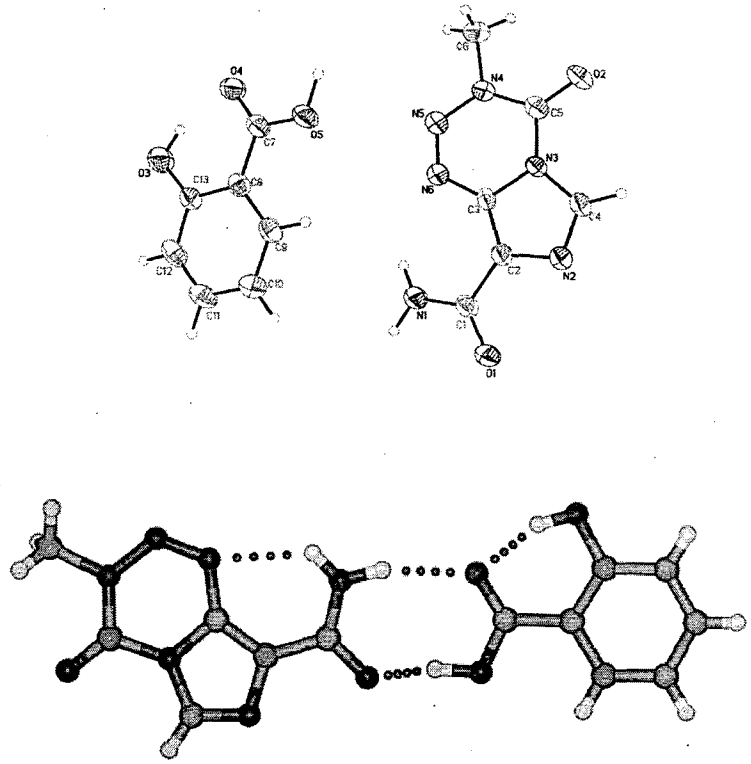
O4
O5
C7
O3
C13
C6
C9
C12
C10
C11
C8
N4
O2
N5
C5
N3
N6
C4
C2
N2
N1
C1
O1

Figure 39

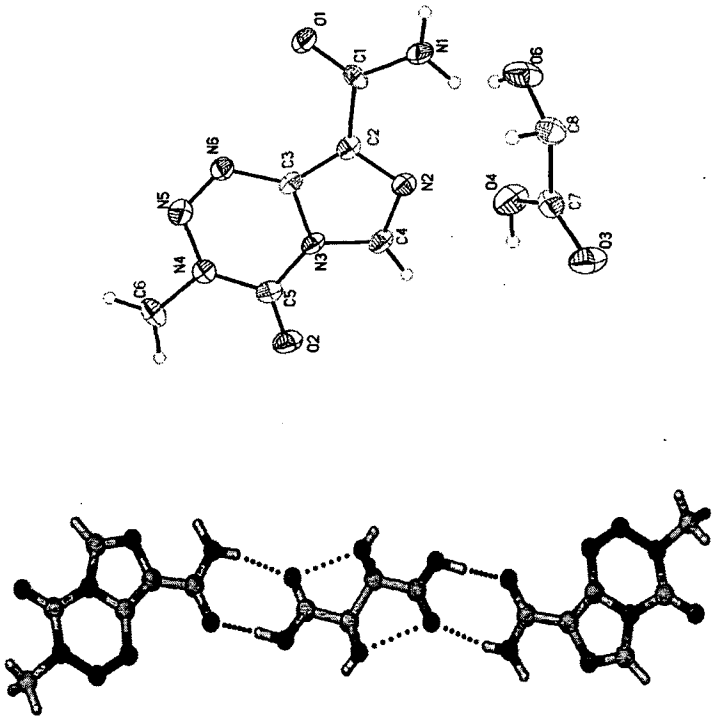

Figure 40

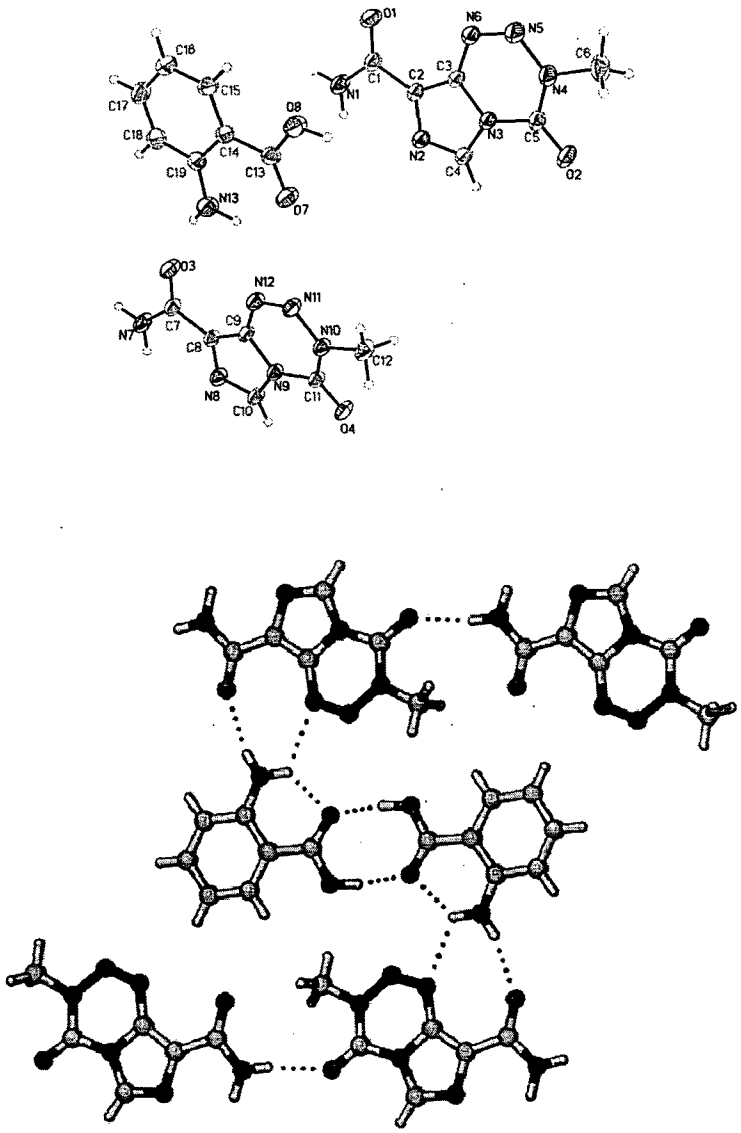
O1
N6
N5
C6
C16
C15
C1
C2
C3
N4
C17
O8
N1
C18
C14
N3
C5
N2
C4
O2
C19
C13
O7
N13
O3
N12
N11
N7
C7
C9
N10
C8
C12
N9
N8
C11
C10
O4

Figure 41

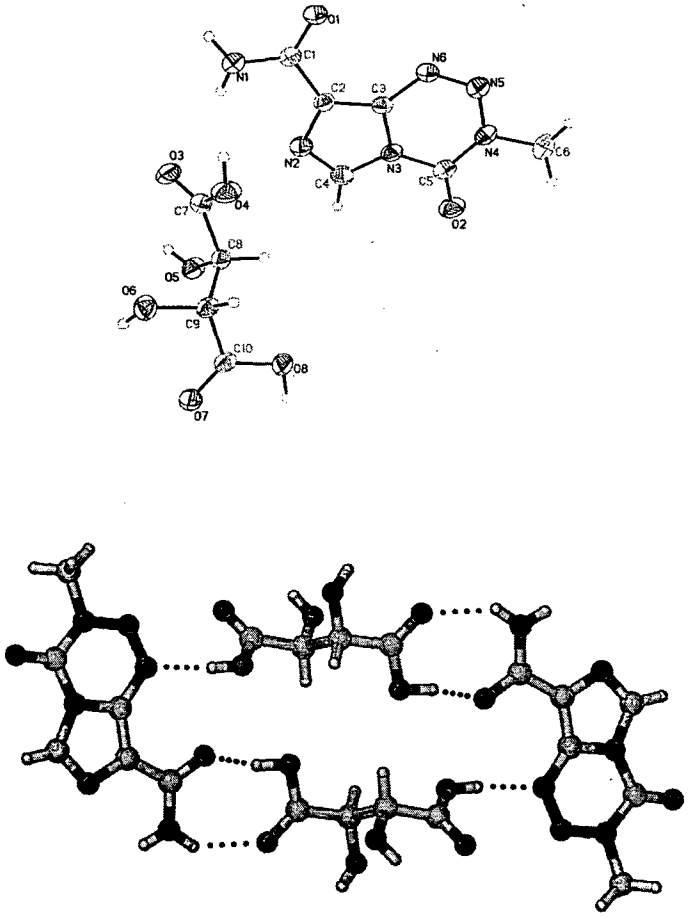

Figure 42

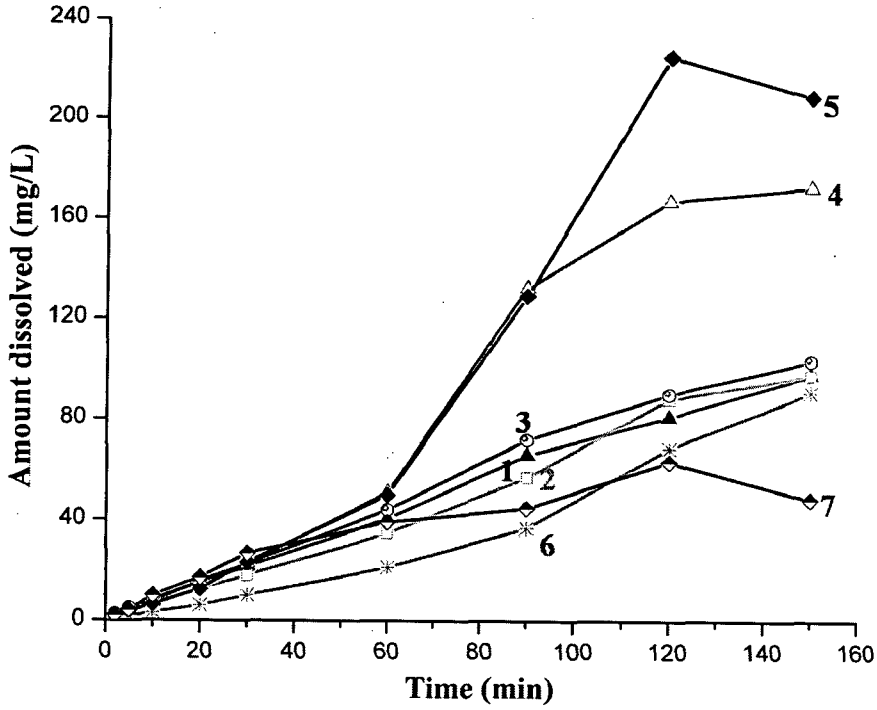
Amount dissolved (mg/L)
240
200
160
120
80
40
0
0
20
40
60
80
100
120
140
160
Time (min)
1
2
3
4
5
6
7

Figure 43